

Journal of Visualized Experiments

Biomechanical testing of murine tendons

--Manuscript Draft--

Article Type:	Methods Article - JoVE Produced Video
Manuscript Number:	JoVE60280R1
Full Title:	Biomechanical testing of murine tendons
Keywords:	3d printing; Additive Manufacturing; tendon; enthesis; biomechanics
Corresponding Author:	Stavros Thomopoulos Columbia University New York, NY UNITED STATES
Corresponding Author's Institution:	Columbia University
Corresponding Author E-Mail:	sat2@columbia.edu
Order of Authors:	Stavros Thomopoulos Iden Kurtaliaj Mikhail Golman Adam C Abraham
Additional Information:	
Question	Response
Please indicate whether this article will be Standard Access or Open Access.	Standard Access (US\$2,400)
Please indicate the city, state/province, and country where this article will be filmed . Please do not use abbreviations.	New York, NY

TITLE:**Biomechanical Testing of Murine Tendons****AUTHORS AND AFFILIATIONS:**

Iden Kurtaliaj^{1,2}, Mikhail Golman^{1,2}, Adam C. Abraham¹, Stavros Thomopoulos^{1,2}

¹Department of Orthopedic Surgery, Columbia University, New York, NY, USA

²Department of Biomedical Engineering, Columbia University, New York, NY, USA

Corresponding Author:

Stavros Thomopoulos (sat2@columbia.edu)

Email Addresses of Co-Authors:

Iden Kurtaliaj (ik2401@columbia.edu)

Mikhail Golman (mg3693@columbia.edu)

Adam C. Abraham (aca2175@cumc.columbia.edu)

KEYWORDS:

3D printing; additive manufacturing; tendon; murine tendons; enthesis; biomechanics

SUMMARY:

The protocol describes efficient and reproducible tensile biomechanical testing methods for murine tendons through the use of custom-fit 3D printed fixtures.

ABSTRACT:

Tendon disorders are common, affect people of all ages, and are often debilitating. Standard treatments, such as anti-inflammatory drugs, rehabilitation, and surgical repair, often fail. In order to define tendon function and demonstrate efficacy of new treatments, the mechanical properties of tendons from animal models must be accurately determined. Murine animal models are now widely used to study tendon disorders and evaluate novel treatments for tendinopathies; however, determining the mechanical properties of mouse tendons has been challenging. In this study, a new system was developed for tendon mechanical testing that includes 3D-printed fixtures that exactly match the anatomies of the humerus and calcaneus to mechanically test supraspinatus tendons and Achilles tendons, respectively. These fixtures were developed using 3D reconstructions of native bone anatomy, solid modeling, and additive manufacturing. The new approach eliminated artifactual gripping failures (e.g., failure at the growth plate failure rather than in the tendon), decreased overall testing time, and increased reproducibility. Furthermore, this new method is readily adaptable for testing other murine tendons and tendons from other animals.

INTRODUCTION:

Tendon disorders are common and highly prevalent among the aging, athletic, and active populations¹⁻³. In the United States, 16.4 million connective tissue injuries are reported each year⁴ and account for 30% of all injury-related physician office visits^{3,5-8}. The most commonly

affected sites include the rotator cuff, Achilles tendon, and patellar tendon⁹. Although a variety of non-operative and operative treatments have been explored, including anti-inflammatory drugs, rehabilitation, and surgical repair, outcomes remain poor, with limited return to function and high rates of failure^{5,6}. These poor clinical outcomes have motivated basic and translational studies seeking to understand tendinopathy and to develop novel treatment approaches.

Tensile biomechanical properties are the primary quantitative outcomes defining tendon function. Therefore, laboratory characterization of tendinopathy and treatment efficacy must include a rigorous testing of tendon tensile properties. Numerous studies have described methods to determine the biomechanical properties of tendons from animal models such as rats, sheep, dogs, and rabbits¹⁰⁻¹². However, few studies have tested the biomechanical properties of murine tendons, primarily due to the difficulties in gripping the small tissues for tensile testing. As murine models have numerous advantages for mechanistically studying tendinopathy, including genetic manipulation, extensive reagent options, and low cost, development of accurate and efficient methods to biomechanically test murine tissues is needed.

In order to properly test the mechanical properties of tendons, the tissue must be gripped effectively, without slipping or artifactual tearing at the grip interface or fracturing of the growth plate. In many cases, particularly for short tendons, the bone is gripped on one end and the tendon is gripped on the other end. Bones are typically secured by embedding them in materials such as epoxy resin¹³ and polymethylmethacrylate^{14,15}. Tendons are often placed between two layers of sandpaper, glued with cyanoacrylate, and secured using compression clamps (if the cross section is flat) or in a frozen medium (if the cross section is large)¹⁵⁻¹⁷. These methods have been applied to biomechanically test murine tendons, but challenges arise due to the small size of the specimens and the compliance of the growth plate, which never ossifies¹⁸. For example, the diameter of the murine humeral head is only a few millimeters, thus making gripping of the bone difficult. Specifically, tensile testing of murine supraspinatus tendon-to-bone samples often results in failure at the growth plate rather than in the tendon or at the tendon enthesis. Similarly, biomechanical testing of the Achilles tendon is challenging. Although the Achilles tendon is larger than other murine tendons, the calcaneus is small, making gripping of this bone difficult. The bone can be removed, followed by gripping the two tendon ends; however, this precludes the testing of the tendon-to-bone attachment. Other groups report gripping the calcaneus bone using custom-made fixtures^{19,20}, anchoring by clamps²¹, fixing in self curing plastic cement²² or using a conical shape slot²², yet these prior methods remain limited by low reproducibility, high gripping failure rates, and tedious preparation requirements.

The objective of the current study was to develop an accurate and efficient method for tensile biomechanical testing of murine tendons, focusing on the supraspinatus and Achilles tendons as examples. Using a combination of 3D reconstructions from native bone anatomy, solid modeling, and additive manufacturing, a novel method was developed to grip the bones. These fixtures effectively secured the bones, prevented growth plate failure, decreased specimen preparation time, and increased testing reproducibility. The new method is readily adaptable to test other murine tendons as well as tendons in rats and other animals.

PROTOCOL:

Animal studies were approved by Columbia University Institutional Animal Care and Use Committee. Mice used in this study were of a C57BL/6J background and were purchased from The Jackson Laboratory (Bar Harbor, ME, USA). They were housed in pathogen-free barrier conditions and were provided food and water ad libitum.

1. Development of custom-fit 3D printed fixtures for gripping bone

1.1. Bone image acquisition and 3D bone model construction

1.1.1. Dissect the bone of interest in preparation for 3D model creation and 3D bone grip printing; the humerus and the calcaneus are used as examples in the current protocol.

NOTE: Detailed instructions to dissect bone-tendon-muscle specimens for mechanical testing are provided in step 2.1.1. The following steps should be followed to isolate bones for the purpose of creating 3D-printed bone grips.

1.1.1.1. Dissection of the humerus: Euthanize a mouse per IACUC-approved procedure. Remove upper extremity skin, remove all muscles over the humerus, disarticulate the elbow and glenohumeral joints, and carefully remove all connective tissues attached to the humerus.

1.1.1.2. Dissection of the calcaneus: Euthanize a mouse per IACUC-approved procedure. Remove lower extremity skin, disarticulate the Achilles tendon-calcaneus joint and joints between calcaneus and other foot bones, and carefully remove all connective tissues attached to the calcaneus.

1.1.2. Perform a microcomputed tomography scan of the entire bone, e.g., scan the humerus and calcaneus samples.

NOTE: Depending on the scanner used, the settings will be different. For the scanner used in the current study (**Table of Materials**), the recommended settings are: scan at an energy of 55 kVP, Al 0.25 filter, at a resolution of 6 μm .

1.1.2.1. Mix agarose powder in ultrapure water and microwave for 1-3 min until the agarose is completely dissolved. It is helpful to microwave for 30-45 s, stop and swirl, and then continue towards a boil. Fill cryotubes up to three-quarters full with agarose. Let the agarose cool for about 5-10 min.

1.1.2.2. Insert bone into the agarose gel (this will prevent movement artifacts during scanning). Insert a cryotube with bone into the scanner.

NOTE: For the scanner used in the current study, a 16-position automatic sample changer was used for all scans. This scanner can automatically select magnification according to a sample's size and shape.

1.1.3. Reconstruct microcomputed tomography scan projection images into cross-section images. Use recommended parameters for the experimenter's scanner/software combination.

NOTE: For the program used in the current study (**Table of Materials**) it is recommended to use the following reconstruction parameters: Smoothing: 0-2, Beam Hardening Correction: 45, Ring Artefact Reduction: 4-9 and to reconstruct slices in 16-bit TIFF format.

1.1.4. Create a 3D surface model and save into a standard STL format compatible with most 3D printers and rapid prototyping. For the program used in the current study (**Table of Materials**), do the following:

1.1.4.1. Select the command **File > Open** to open the file dataset. Open the dialog **File > Preferences** and select the **Advanced** tab.

1.1.4.2. Use the double-time cubes algorithm to construct the 3D models. This algorithm minimizes the number of facet triangles and provides smoother surface detail. Use 10 as the locality parameter; this parameter defines the distance in pixels to the neighboring point used for finding the object border. Minimize tolerance to 0.1 to decrease file size.

NOTE: After opening the dataset, the images are shown in the "Raw Images" page.

1.1.4.3. To specify the volume of interest (VOI), manually select two images to set as the top and bottom of the selected VOI range.

1.1.4.4. Move to the second page, **Region of Interest**. Manually select the region of interest on a single cross section image.

NOTE: The selected region will be highlighted in red (i.e., the humerus cross-sectional area).

1.1.4.5. Repeat the previous step every 10–15 cross-section images.

1.1.4.6. Move to the third page **Binary Selection**. On the histogram menu, click **From dataset**. The histogram distribution of brightness from all images of the dataset will be shown. Also on the histogram menu, click the **Create a 3D Model** file menu.

1.1.5. Save a 3D model of the bone in STL file format.

1.1.6. Refine the mesh: Manipulate the mesh to reduce the size of the STL file and make it compatible with any solid modeling computer-aided design program. For the program used in the current study (**Table of Materials**), follow the steps below:

1.1.6.1. Choose **Refine Mesh** from the toolset **Utilities**. Select the mesh object to edit. Reduce mesh by a factor of 0.95 to lower the end size of the mesh object. Resave the newly reduced file in STL format by choosing **Export as....**

NOTE: The “Remesh” tool could also be used to reduce the size of the mesh.

1.2. Design of custom-fit bone fixtures

1.2.1. Supraspinatus tendon-humeral bone

1.2.1.1. Use a solid modeling computer-aided design program to create a custom-fit model of humerus gripping fixture (**Figure 1, Supplemental Files**).

NOTE: The program used in the current study is listed in the **Table of Materials**.

1.2.1.2. Open the STL format file of the humerus bone in a solid modeling program and save as a part file.

NOTE: For the software used in the current study (**Table of Materials**), the 3D bone object was saved in SLDPRT format.

1.2.1.3. Open the part file and manually create three anatomically relevant planes (i.e., sagittal, coronal, transverse).

1.2.1.3.1. Manually define the sagittal plane to cut through the supraspinatus tendon attachment at the greater tuberosity. Ensure that the 3D block contains the sagittal plane as a plane of symmetry. To achieve this, add or cut material from the block if needed.

NOTE: This plane of symmetry ensures that when the specimen is inserted into the fixtures the tendon and tendon attachment are located in the central axis of the fixture.

1.2.1.4. Measure dimensions of the bone along each of the three planes (i.e., height, width, length).

1.2.1.5. Measure the dimensions of the mechanical testing grips where the 3D printed fixture will be attached.

1.2.1.6. Begin by designing a solid block part (e.g., a solid cylinder).

1.2.1.6.1. Ensure that each dimension of the block is at least 5 mm greater than the dimensions of the humerus.

1.2.1.6.2. Account for design constraints from mechanical testing grips (i.e., ensure that the 3D printed fixture can be assembled and disassembled freely in the mechanical testing grips).

1.2.1.7. Create an assembly model with two components: the solid block and either the right or left humerus bone. Define the orientation of the bone within the block (i.e., the angle between the tendon and bone). Ensure that the entire bone volume fits inside the block.

1.2.1.8. Create a cavity in the block using the humerus bone as the mold. If using the software specified in the **Table of Materials**, follow the following steps:

1.2.1.8.1. Insert the design part (humerus) and the mold base (cylinder block) into an interim assembly. In the assembly window, select the block, and click **Edit Component** from the **Assembly** toolbar.

1.2.1.8.2. Click **Insert > Mold > Cavity**. Select Uniform scaling and enter 0% as the value to scale in all directions.

1.2.1.9. Cut the assembly along the sagittal plane to create two symmetrical components that fit the bone anteriorly and posteriorly (e.g., two half cylinders, as seen in **Figure 1**).

NOTE: Two components are designed that fit the bone anteriorly and posteriorly. The anterior component includes a half spherical-shaped cavity extended from the anterior side of the humeral head up to the supraspinatus tendon attachment. The posterior component cavity is shaped like the posterior part of the humerus (i.e., posterior side of the humeral head, deltoid tuberosity, and medial and lateral epicondyle).

1.2.1.10. Save each component as a separate file part.

1.2.1.11. For the anterior component, ensure that the humeral head is embedded in the cavity of the part by defining appropriate tolerances.

NOTE: In the current study, using the software specified in the **Table of Materials**, it is suggested to follow the steps below:

1.2.1.11.1. Create a revolved cut to smooth the mesh geometry of the cavity. Create a sketch for the cut by emulating the cavity geometry and adding a locational clearance.

NOTE: The clearance allows for free assembly and disassembly between the bone and the anterior component.

1.2.1.12. Modify the posterior component to imitate the cavity geometry to create a cut that adds clearance, as described above for the anterior component.

1.2.1.13. Make a cut in the transverse plane starting from the top of the posterior component up to the crest of the greater/lesser tubercle.

NOTE: As seen in **Figure 1** and **Figure 2**, the posterior component includes a cut that creates an opening at the tendon attachment.

1.2.1.14. Create a snug fit between the two components to allow for free assembly and disassembly.

NOTE: A hole-shaft fit with a loose running clearance was created for the fixtures in the current study.

1.2.1.15. Create 3D mirror models for each component of the fixture for the opposite limb (i.e., left or right).

1.2.1.16. Add an etch on the bottom of the fixtures to distinguish between the left and right sides.

1.2.1.17. Save all fixture parts in STL standard file format in preparation for 3D printing.

1.2.2. Achilles tendon-calcaneus bone

1.2.2.1. Follow the same steps as described above for supraspinatus-humeral head fixture.

NOTE: Only one set of fixtures is necessary for the Achilles-calcaneal, since the anatomy of the left and right calcaneus bones is nearly symmetrical.

2. Biomechanical testing of murine tendons

2.1. Specimen preparation and cross-sectional area measurement

2.1.1. Dissect the muscle-tendon-bone of interest in preparation for tensile mechanical testing.

In the current study, supraspinatus muscle - tendon - humerus bone specimens (N=10, 5 male, 5 female) and gastrocnemius muscle - Achilles tendon-calcaneus bone specimens (N=12, 6 male, 6 female) were isolated from 8 week old C57BL/6J mice.

2.1.1.1. Dissection of the supraspinatus muscle - tendon - humerus bone specimen

2.1.1.1.1. Euthanize a mouse per IACUC-approved procedure. Position the mouse in a prone position. Make an incision in the skin from above the elbow of the forepaw towards the shoulder.

2.1.1.1.2. Carefully remove the skin with blunt dissection so that the musculature of the shoulder is visible. Remove the tissue surrounding the humerus until the bone is exposed and can be held securely with forceps.

2.1.1.1.3. Hold the humerus with forceps and carefully remove the deltoid and trapezius muscles to expose the coracoacromial arch. Identify the acromioclavicular joint and carefully separate the clavicle from the acromion with a scalpel blade.

2.1.1.1.4. Taking care not to damage the supraspinatus tendon and its bony attachment, remove the muscle from its scapular attachment using a scalpel blade. Taking care not to damage the supraspinatus tendon and its bony attachment, detach the humeral head from the glenoid; using a scalpel blade, lacerate the joint capsule and the infraspinatus, subscapularis, and teres minor tendons.

2.1.1.1.5. Disarticulate the elbow joint to separate the humerus from the ulna and radius. Isolate the humerus - supraspinatus tendon - muscle specimen and clean off excess soft tissues on the humerus and humeral head.

2.1.1.2. Dissection of the Achilles tendon - calcaneus bone sample

2.1.1.2.1. Euthanize a mouse per IACUC-approved procedure. Position the mouse in a supine position. Taking care not to damage the Achilles tendon and its bony attachment, remove the skin with blunt dissection so that the musculature around the ankle and knee joints is exposed.

2.1.1.2.2. Using a scalpel blade, starting at the Achilles tendon - calcaneus attachment, carefully detach the gastrocnemius muscle from its proximal attachments.

2.1.1.2.3. Carefully disarticulate the calcaneus from the various adjacent bones. Isolate the Achilles tendon - calcaneus specimen and clean off excess soft tissues.

2.1.2. Determine the cross-sectional area of the tendon using microcomputed tomography.

NOTE: For the scanner used in the current study (**Table of Materials**), the recommended settings are: scan at an energy of 55 kVP, Al 0.25 filter, at a resolution of 5 μm .

2.1.2.1. Mix agarose powder in ultrapure water and microwave for 1-3 min until the agarose is completely dissolved. It is helpful to microwave for 30-45 s, stop and swirl, and then continue towards a boil. Fill cryotubes up to three-quarters full with agarose. Let the agarose cool for about 5-10 min.

2.1.2.2. Suspend the specimen in the cryotube by inserting the bone upside down.

NOTE: Only the bone should be in the agarose gel. The tendon and muscle should be suspended outside.

2.1.3. After the scan, gently remove muscle from tendon using scalpel blade. Insert the specimen into the 3D-printed fixture.

NOTE: The grips are reusable for each test. Do not use glue or epoxy in the fixture; the bone is held in a press fit.

2.1.4. Insert and glue the tendon between a folded thin tissue paper (2 cm x 1 cm) and clamp the construct using thin film grips. Attach a 3D printed fixture with the specimen into the testing grips.

2.1.5. Insert the sample and the grips into a testing bath of phosphate buffered saline (PBS) at 37 °C (i.e., mouse body temperature²³).

2.2. Tensile testing

2.2.1. Perform tensile mechanical test on a material testing frame.

NOTE: For the testing frame used in the current study (**Table of Materials**), the recommended protocol is:

2.2.1.1. Define the gauge length as the distance from the tendon attachment to the upper grip.

2.2.1.2. Precondition with 5 cycles between 0.05 N and 0.2 N.

2.2.1.3. Hold for 120 s.

2.2.1.4. Use a tension to failure of 0.2%/s.

2.2.2. Collect load-deformation data.

2.2.3. Calculate the strain as the displacement relative to the initial gauge length of the tendon.

2.2.4. Calculate the stress as the force divided by the initial tendon cross-sectional area (as measured from microCT).

2.2.5. If interested in viscoelastic behavior, perform a stress relaxation prior to the tension test to failure and use the data to calculate parameters such as A, B, C, tau1, and tau2 from the quasilinear viscoelastic model²⁴.

2.2.6. From the load deformation curve, calculate the stiffness (slope of linear portion of curve), the maximum force, and the work to yield (the area under the curve up to yield force).

2.2.6.1. Identify the linear portion by choosing a window of points in the load-deformation curve that maximizes the R2 value for a linear least squares regression²⁵.

2.2.6.2. Determine the stiffness as the slope of the linear portion of the load-displacement curve^{25,26}.

2.2.7. From the stress strain curve, calculate the modulus (slope of linear portion of curve), the strength (maximum stress), and the resilience (area under the curve up to yield stress).

NOTE: Using the RANSAC algorithm, the yield strain (x-value) is defined as the first point when the y-fit has deviated more than 0.5% of the expected stress value (y-value). Yield stress is the corresponding y-value of the yield strain.

NOTE: In addition to the monotonic tensile loading to failure described in the current study, cyclic loading can provide important information about tendon fatigue and/or viscoelastic properties. For example, Freedman et al. reported fatigue properties of the murine Achilles tendons²⁷.

2.2.8. After completion of tensile testing, perform a microcomputed tomography scan of the entire bone, e.g., scan the humerus and calcaneus samples.

NOTE: For the scanner used in the current study (**Table of Materials**), the recommended settings are: scan at an energy of 55 kVP, Al 0.25 filter, at a resolution of 6 μm .

2.2.8.1. Repeat steps 1.1.2.1–1.1.2.2.

2.2.9. Repeat step 1.1.3.

2.2.10. Use a 3D visualization program compatible with the scanner to create a volume-rendered 3D model of the scanned object.

NOTE: The program used in the current study is listed in the **Table of Materials**.

2.2.11. Determine the failure mode and failure site area by inspecting the 3D object.

2.3. Statistical analysis: Show all sample results as mean \pm standard deviation (SD). Make comparisons between groups using student's t-tests (two-tailed and unpaired). Set significance as $p < 0.05$.

NOTE: The statistical software used in the current study is listed in the **Table of Materials**.

REPRESENTATIVE RESULTS:

3D-printed fixtures were used to test 8-week old murine supraspinatus and Achilles tendons. All mechanically tested samples failed at the enthesis, as characterized by microCT scans, visual inspection, and video analysis after tensile tests. A one-to-one comparison of the previous and current methods for supraspinatus tendon testing in our laboratory is shown in **Figure 3**. In the previous method^{28–30}, the humerus bone was embedded in epoxy and a paper clip was placed over the humeral head in an effort to prevent growth plate fracture. 4-6 hours were necessary to allow for the epoxy to fully cure (**Figure 3**), allowing for only 6-8 specimens to be tested in a typical day. A further limitation of the approach was the user-dependent effectiveness of the paper clip placement for preventing growth plate fracture. The testing results using these prior methods were highly variable, with coefficients of variation on the order of 30% for most parameters and growth plate failure rates of approximately 10%–20%. As summarized in **Figure**

3, specimen preparation time using the new methods was decreased to 5–10 minutes, making it practical to test 16–20 samples per day. Furthermore, growth plate failures were eliminated.

Compared to methodology reported by others for testing murine tendons^{14,15,17,25,28–33}, the new methods were more efficient and reproducible. For supraspinatus tendons, structural properties such as maximum load (3.8 ± 0.6 N) and stiffness (12.7 ± 1.8 N/mm), as well as normalized material properties such as maximum stress (10.4 ± 3.3 MPa), and modulus (51.7 ± 13.5 MPa) had considerably lower coefficients of variations compared to results from the literature (**Table 1**). For the Achilles tendon, mechanical properties such as maximum load (7.8 ± 1.1 N) and stiffness (13.2 ± 1.9 N/mm) had lower coefficients of variations compared to results from the literature^{19,21,22,32–38}, whereas maximum stress (24.2 ± 5.4 MPa) and modulus (52.5 ± 22.5 MPa) had coefficients of variations similar to those reported in the literature (**Table 2**).

Animal sex had a significant effect on the mechanical properties of the supraspinatus and Achilles tendons (**Figure 4**). When comparing male and female supraspinatus tendons, there were significant increases in maximum force ($p = 0.002$) and work to yield ($p = 0.008$). There were trends between the two groups for stiffness ($p = 0.057$), stress ($p = 0.068$), modulus ($p = 0.061$) and resilience ($p = 0.078$). When comparing male and female Achilles tendons, there were significant increases in maximum stress ($p = 0.0006$) and resilience ($p = 0.0019$). There were trends between the two groups for work to yield ($p = 0.079$), and modulus ($p = 0.074$). There was no difference between the two groups for maximum force ($p = 0.1880$) and stiffness ($p = 0.6759$).

FIGURE AND TABLE LEGENDS:

Figure 1: Representative 3D models of fixtures for the humerus (top row) and the calcaneus (bottom row). (A) 3D models of the bones. (B) Disassembled models of the fixtures. (C) Assembled models of the fixtures. The supraspinatus tendon attachment is indicated by arrows.

Figure 2: Representative 3D printed fixtures. (A) Fixture for biomechanical testing of supraspinatus tendons of 8-week old mice at an angle between the humerus and supraspinatus tendon of 180°. (B) Fixture for biomechanical testing of supraspinatus tendons of 8-week old mice at an angle between the humerus and supraspinatus tendon of 135°. (C) Fixture for biomechanical testing of murine Achilles tendons at an angle between the calcaneus and Achilles tendon of 120°. (D) Fixture for biomechanical testing of supraspinatus tendons of adult Sprague Dawley rats at an angle between the humerus and supraspinatus tendon of 180°. Scale bar: 5 mm.

Figure 3: Comparison of previous and current methods for mechanical testing of murine supraspinatus tendons. (A) Previous specimen preparation methods used in our laboratory prior to mechanical testing: the humerus was potted in epoxy up to the humeral head to stabilize the bone, a paper clip was placed over the humeral head to prevent growth plate fracture, and, for the epoxy to cure, the specimens were left in room temperature for 4–6 hours prior to mechanical testing. (B) Specimen preparation methods used in the current study (Steps 1.2 and 2.1.4): Top left shows a 3D representation of the fixtures as produced by a solid modeling program. The 3D

printed fixtures are reusable and easily assembled and disassembled. The bone end of the specimen is inserted into the fixtures, securing the growth plate and exposing the tendon for gripping and testing. The tendon end is glued between a folded thin tissue paper and inserted into the grips. Preparation time for each specimen is 10–15 minutes. (C) Representative load-deformation curves for tensile testing of supraspinatus tendon using current methods. (D) Representative load-deformation curve for tensile testing of supraspinatus tendon showing a growth plate failure.

Figure 4: Sex effect on the mechanical properties of supraspinatus (SST) and Achilles (AHT) tendons. There was a significant effect of sex on many of the mechanical properties based on unpaired t-tests (*sex effect, $p < 0.05$). Data shown as mean \pm standard deviation.

Figure 5: Cross-sectional area measurement from microCT. (A) Minimum cross-sectional area measurement along the length of supraspinatus tendon. (B) Minimum cross-sectional area measurement along the length of Achilles tendon. Only the tendon proper should be selected for measurement.

Table 1: Mechanical properties of supraspinatus tendons. Mean \pm SD and coefficient of variation (COV) for structural and material properties estimated using new methods compared to ones reported in the literature. [NR: not reported, * estimated from figure(s), # standard deviation calculated from reported standard error, † measured deformation using optical stain lines].

Table 2: Mechanical properties of Achilles tendons. Mean \pm SD and COV for structural and material properties estimated using new methods compared to ones reported in the literature. [NR: not reported, * estimated from figure(s), # standard deviation calculated from reported standard error].

DISCUSSION:

Murine animal models are commonly used to study tendon disorders, but characterization of their mechanical properties is challenging and uncommon in the literature. The purpose of this protocol is to describe a time efficient and reproducible method for tensile testing of murine tendons. The new methods reduced the time required to test a sample from hours to minutes and eliminated a major gripping artifact that was a common problem in previous methods.

Several steps described in this protocol are critical to produce effective fixtures mechanically testing murine supraspinatus and Achilles tendons. First, step 1.1.2 is necessary to create a 3D model of the desired bone; however, due to the typically high resolution used for this scan, the file size may be too large to use with solid modeling programs. The software used in this protocol successfully reduced the size of the file (step 1.1.6) and preserved object geometry, although other software may also be effective to achieve this. Second, each anatomic site has specific design criteria to consider for effective gripping. For the design of the supraspinatus tendon fixture, it is critical to: (i) secure the humeral head to prevent growth plate failure (step 1.2.1.11), (ii) define a clearance fit that avoids disengaging of the humerus bone from the mold during testing (step 1.2.1.11.2) and (iii) orient the humerus bone to form a 180° angle with the long axis

of the tendon (step 1.2.1.7). For the Achilles tendon fixture design, it is critical to: (i) define a clearance fit that grips the small calcaneus bone without slipping out from the fixture during testing and (ii) orient the calcaneus bone to form a 120° angle (30° plantar flexion) with the long axis of the tendon. Third, accurate measurement of the tendon cross-sectional area (step 2.1.2) is critical to properly calculate engineering stress for determination of material properties. To measure the cross-sectional area of the supraspinatus tendon, we recommend microcomputed tomography scans of the bone-tendon-muscle specimen suspended in a cryotube with a flat bottom, with the bone held upside down in the tube with agarose. Only the humerus bone should be inserted into the agarose gel, while the humeral head with the tendon and muscle attached should be scanned in air. As the supraspinatus tendon has a splayed geometry as it inserts into the bone, the most consistent way to measure the cross-sectional area is to determine the minimum cross-sectional area along the length of the tendon. A similar procedure should be followed to measure the cross-sectional area of the Achilles tendon. For the Achilles tendon, high resolution microcomputed tomography scans reveal two distinct tissues: the tendon proper and the surrounding sheath, which appears as a lighter shade. To consistently estimate the minimal cross-sectional area for the Achilles tendon, only the tendon proper should be selected for measurement (**Figure 5**). Lastly, the grips are reusable and small variations from sample to sample do not affect their effectiveness. Each bone should be scanned once (e.g., for the current study, left humerus, right humerus, and calcaneus) and one 3D model should be created for each bone. In addition, for animals of the same age, the bone geometry is nearly identical, thus the same fixture can be used for testing of all specimens. In this manuscript, 3D printed fixtures specific to 8-week old mice (skeletally mature adult mice) were used to test tendons. It was not necessary to create separate male and female fixtures. For other age groups (e.g., 4-week old mice) or mice with unique bone phenotypes, it is recommended that fixtures that fit the particular geometries of the bones are manufactured.

After design and 3D printing of the fixtures, to ensure reproducibility and efficiency of the approach, 10 tendon samples from mice of the same background, age, and sex of the planned study should typically be tested (the exact sample size may vary depending on the tissue and animal model). The mechanical properties of these tendons should be determined to ensure that coefficients of variation for structural and material properties are within the expected range, as described in **Table 1** and **Table 2**. These pilot tests should also confirm that artifactual failures (e.g., growth plate failure) do not occur. Multiple cycles of design, prototyping, and validation may be needed to achieve the desired results for tendons other than the supraspinatus and Achilles tendons described in the current paper.

A number of groups have reported the mechanical properties of murine tendons. The coefficient of variations in these studies are typically high, often making it difficult to pick up differences among the comparison groups. Furthermore, methodological differences in tissue gripping among the various studies makes it difficult to determine whether failure properties are relevant to tendon or due to artifactual grip failures. To compare the new testing methods with existing methodologies, a literature review was performed and the results from 20 studies were summarized (**Table 1** and **Table 2**). For supraspinatus tendon mechanical testing, the average coefficients of variation for maximum force, stiffness, maximum stress, and modulus were 27%,

39%, 52%, and 45%, respectively. For Achilles tendon mechanical testing, the average coefficients of variation for maximum force, stiffness, maximum stress, and modulus were 14%, 14%, 22%, and 22%, respectively. In the current study, the new method for testing murine tendons resulted in a 27%–52% reduction of supraspinatus tendon coefficients of variation and 6%–39% reduction in Achilles tendon coefficients of variation.

There is no current standard methodology for gripping bones, thus it is unclear to what extent artifactual gripping issues has affected reported mechanical properties of murine tendons. Most groups report gripping the humerus bone by using epoxy resin¹³, polymethylmethacrylate (PMMA)^{14,15}, or cyanoacrylate¹⁶ and securing the humeral head by applying a second coating of PMMA¹⁴, using custom fixture³⁹ and/or inserting a paper clip^{25,28,30}. Similarly, other groups report gripping of the much smaller calcaneus bone using custom-made fixtures^{19,20}, anchoring by clamps²¹, fixing in self curing plastic cement²² or using a conical shape slot²². However, these methods remain limited by low reproducibility, high artifactual failure rates, and time-consuming preparation requirements. The new methods presented in this study have eliminated artifactual grip failures and have tripled the number of specimens that can be tested in a day. Furthermore, these methods are not limited to the supraspinatus and Achilles tendons, as they are easily adapted to testing other murine tendons and tendons from larger animal models. To test tendons from larger animals, however, the modulus of the 3D printed fixture material must be high enough that it is not compliant relative to the strength of the tendon being tested.

In the current study, sex had a significant effect on the mechanical properties of murine tendons. As guided by the National Institutes of Health (NIH), we recommend accounting for sex as a biological variable in the research design of animal models where tendon mechanical properties will be measured. There are sex-based differences in tendon disorders, with several studies indicating that women have reduced function following treatment after tendon injury^{40–42}.

ACKNOWLEDGMENTS:

The study was supported by the NIH / NIAMS (R01 AR055580, R01 AR057836).

DISCLOSURES:

The authors have nothing to disclose.

REFERENCES:

1. Girish, N., Ramachandra, K., Arun G, M., Asha, K. Prevalence of Musculoskeletal Disorders Among Cashew Factory Workers. *Archives of Environmental & Occupational Health*. **67**, 37–42 (2012).
2. Thomopoulos, S., Parks, W. C., Rifkin, D. B., Derwin, K. A. Mechanisms of tendon injury and repair. *Journal of Orthopaedic Research*. **33**, 832–839 (2016).
3. Scott, A., Ashe, M. C. Common Tendinopathies in the Upper and Lower Extremities. *Current Sports Medicine Reports*. **5**, 233–241 (2006).
4. Praemer, A., Furner, S., Rice, D. P. *Musculoskeletal Conditions in the United States*. American Academy of Orthopaedic Surgeons (American Academy of Orthopaedic Surgeons, 1992).

- 615 5. Nourissat, G., Berenbaum, F., Duprez, D. Tendon injury: From biology to tendon repair.
616 *Nature Reviews Rheumatology*. **11**, 223–233 (2015).
- 617 6. Galatz, L. M., Ball, C. M., Teefey, S. A., Middleton, W. D., Yamaguchi, K. The outcome and
618 repair integrity of completely arthroscopically repaired large and massive rotator cuff
619 tears. *The Journal of Bone and Joint Surgery*. **86**, 219–224 (2004).
- 620 7. Sher, J. S., Uribe, J. W., Posada, A., Murphy, B. J., Zlatkin, M. B. Abnormal findings on
621 magnetic resonance images of asymptomatic shoulders. *The Journal of Bone and Joint
622 Surgery*. **77**, 10–15 (1995).
- 623 8. Ker, R. F., Wang, X. T., Pike, A. V. Fatigue quality of mammalian tendons. *The Journal of
624 Experimental Biology*. **203**, 1317–27 (2000).
- 625 9. Wilson, J. J., Best, T. M. Common overuse tendon problems: A review and
626 recommendations for treatment. *American Family Physician*. **72**, 811–8 (2005).
- 627 10. Fleischer, J. et al. Biomechanical strength and failure mechanism of different tubercula
628 refixation methods within the framework of an arthroplasty for shoulder fracture.
629 *Orthopaedics & Traumatology: Surgery & Research*. **103**, 165–169 (2017).
- 630 11. West, J. R., Juncosa, N., Galloway, M. T., Boivin, G. P., Butler, D. L. Characterization of in
631 vivo Achilles tendon forces in rabbits during treadmill locomotion at varying speeds and
632 inclinations. *Journal of Biomechanics*. **37**, 1647–1653 (2004).
- 633 12. Cavinatto, L. et al. Early versus late repair of rotator cuff tears in rats. *Journal of Shoulder
634 and Elbow Surgery*. **27**, 606–613 (2018).
- 635 13. Potter, R., Havlioglu, N., Thomopoulos, S. The developing shoulder has a limited capacity
636 to recover after a short duration of neonatal paralysis. *Journal of Biomechanics*. **47**, 2314–
637 2320 (2014).
- 638 14. Connizzo, B. K., Sarver, J. J., Iozzo, R. V., Birk, D. E., Soslowky, L. J. Effect of Age and
639 Proteoglycan Deficiency on Collagen Fiber Re-Alignment and Mechanical Properties in
640 Mouse Supraspinatus Tendon. *Journal of Biomechanical Engineering*. **135**, 021019 (2013).
- 641 15. Beason, D. P. et al. Hypercholesterolemia increases supraspinatus tendon stiffness and
642 elastic modulus across multiple species. *Journal of Shoulder and Elbow Surgery*. **22**, 681–
643 686 (2013).
- 644 16. Miller, K. S., Connizzo, B. K., Soslowky, L. J. Collagen fiber re-alignment in a neonatal
645 developmental mouse supraspinatus tendon model. *Annals of Biomedical Engineering*. **40**,
646 1102–1110 (2012).
- 647 17. Cong, G. T. et al. Evaluating the role of subacromial impingement in rotator cuff
648 tendinopathy: Development and analysis of a novel murine model. *Journal of Orthopaedic
649 Research*. **36**, 2780–2788 (2018).
- 650 18. Thomopoulos, S., Birman, V., Genin, G. M. *Structural Interfaces and Attachments in
651 Biology. Infection and Immunity*. **35**, (Springer, 2013).
- 652 19. Boivin, G. P. et al. Biomechanical properties and histology of db/db diabetic mouse Achilles
653 tendon. *Muscles, Ligaments and Tendons Journal*. **4**, 280–284 (2014).
- 654 20. Ansoorge, H. L., Adams, S., Birk, D. E., Soslowky, L. J. Mechanical, Compositional, and
655 Structural Properties of the Post-natal Mouse Achilles Tendon. *Annals of Biomedical
656 Engineering*. **39**, 1904–1913 (2011).
- 657 21. Shu, C. C., Smith, M. M., Appleyard, R. C., Little, C. B., Melrose, J. Achilles and tail tendons
658 of perlecan exon 3 null heparan sulphate deficient mice display surprising improvement in

- tendon tensile properties and altered collagen fibril organisation compared to C57BL/6 wild type mice. *PeerJ*. **6**, e5120 (2018).
22. Probst, A. et al. A new clamping technique for biomechanical testing of tendons in small animals. *Journal of Investigative Surgery*. **13**, 313–318 (2000).
23. Talan, M. Body temperature of C57BL/6J mice with age. *Experimental Gerontology*. **19**, 25–29 (1984).
24. Newton, M. D. et al. The influence of testing angle on the biomechanical properties of the rat supraspinatus tendon. *Journal of Biomechanics*. **49**, 4159–4163 (2016).
25. Schwartz, A. G., Lipner, J. H., Pasteris, J. D., Genin, G. M., Thomopoulos, S. Muscle loading is necessary for the formation of a functional tendon enthesis. *Bone*. **55**, 44–51 (2014).
26. Gimbel, J. A., Kleunen, J. P. Van, Williams, G. R., Thomopoulos, S., Soslowsky, L. J. Long durations of immobilization in the rat result in enhanced mechanical properties of the healing supraspinatus tendon. *Journal of Biomechanical Engineering*. **129**, 400–404 (2006).
27. Freedman, B. R., Sarver, J. J., Buckley, M. R., Voleti, P. B., Soslowsky, L. J. Biomechanical and structural response of healing Achilles tendon to fatigue loading following acute injury. *Journal of Biomechanics*. **47**, 2028–2034 (2014).
28. Deymier, A. C. et al. The multiscale structural and mechanical effects of mouse supraspinatus muscle unloading on the mature enthesis. *Acta Biomaterialia*. **83**, 302–313 (2019).
29. Killian, M. L., Thomopoulos, S. Scleraxis is required for the development of a functional tendon enthesis. *FASEB Journal*. **30**, 301–311 (2016).
30. Schwartz, A. G., Long, F., Thomopoulos, S. Enthesis fibrocartilage cells originate from a population of Hedgehog-responsive cells modulated by the loading environment. *Development*. **142**, 196–206 (2015).
31. Bell, R., Taub, P., Cagle, P., Flatow, E. L., Andarawis-Puri, N. Development of a mouse model of supraspinatus tendon insertion site healing. *Journal of Orthopaedic Research*. **33**, 25–32 (2014).
32. Connizzo, B. K., Bhatt, P. R., Liechty, K. W., Soslowsky, L. J. Diabetes Alters Mechanical Properties and Collagen Fiber Re-Alignment in Multiple Mouse Tendons. *Annals of Biomedical Engineering*. **42**, 1880–1888 (2014).
33. Eekhoff, J. D. et al. Functionally Distinct Tendons From Elastin Haploinsufficient Mice Exhibit Mild Stiffening and Tendon-Specific Structural Alteration. *Journal of Biomechanical Engineering*. **139**, 111003 (2017).
34. Mikic, B., Bierwert, L., Tsou, D. Achilles tendon characterization in GDF-7 deficient mice. *Journal of Orthopaedic Research*. **24**, 831–841 (2006).
35. Sikes, K. J. et al. Knockout of hyaluronan synthase 1, but not 3, impairs formation of the retrocalcaneal bursa. *Journal of Orthopaedic Research*. **36**, 2622–2632 (2018).
36. Wang, V. M., Banack, T. M., Tsai, C. W., Flatow, E. L., Jepsen, K. J. Variability in tendon and knee joint biomechanics among inbred mouse strains. *Journal of Orthopaedic Research*. **24**, 1200–1207 (2006).
37. Wang, V. M. et al. Murine tendon function is adversely affected by aggrecan accumulation due to the knockout of ADAMTS5. *Journal of Orthopaedic Research*. **30**, 620–626 (2011).
38. Zhang, K. et al. Tendon mineralization is progressive and associated with deterioration of tendon biomechanical properties, and requires BMP-Smad signaling in the mouse Achilles

tendon injury model. *Matrix Biology*. **52–54**, 315–324 (2016).

39. Rooney, S. I. et al. Ibuprofen differentially affects supraspinatus muscle and tendon adaptations to exercise in a rat model. *American Journal of Sports Medicine*. **44**, 2237–2245 (2016).

40. Galasso, O. et al. Quality of Life and Functional Results of Arthroscopic Partial Repair of Irreparable Rotator Cuff Tears. *Arthroscopy - Journal of Arthroscopic and Related Surgery*. **33**, 261–268 (2017).

41. Sarver, D. C. et al. Sex differences in tendon structure and function. *Journal of Orthopaedic Research*. **35**, 2117–2126 (2017).

42. Razmjou, H. et al. Disability and satisfaction after Rotator Cuff decompression or repair: A sex and gender analysis. *BMC Musculoskeletal Disorders*. **12**, 66 (2011).

Figure 1

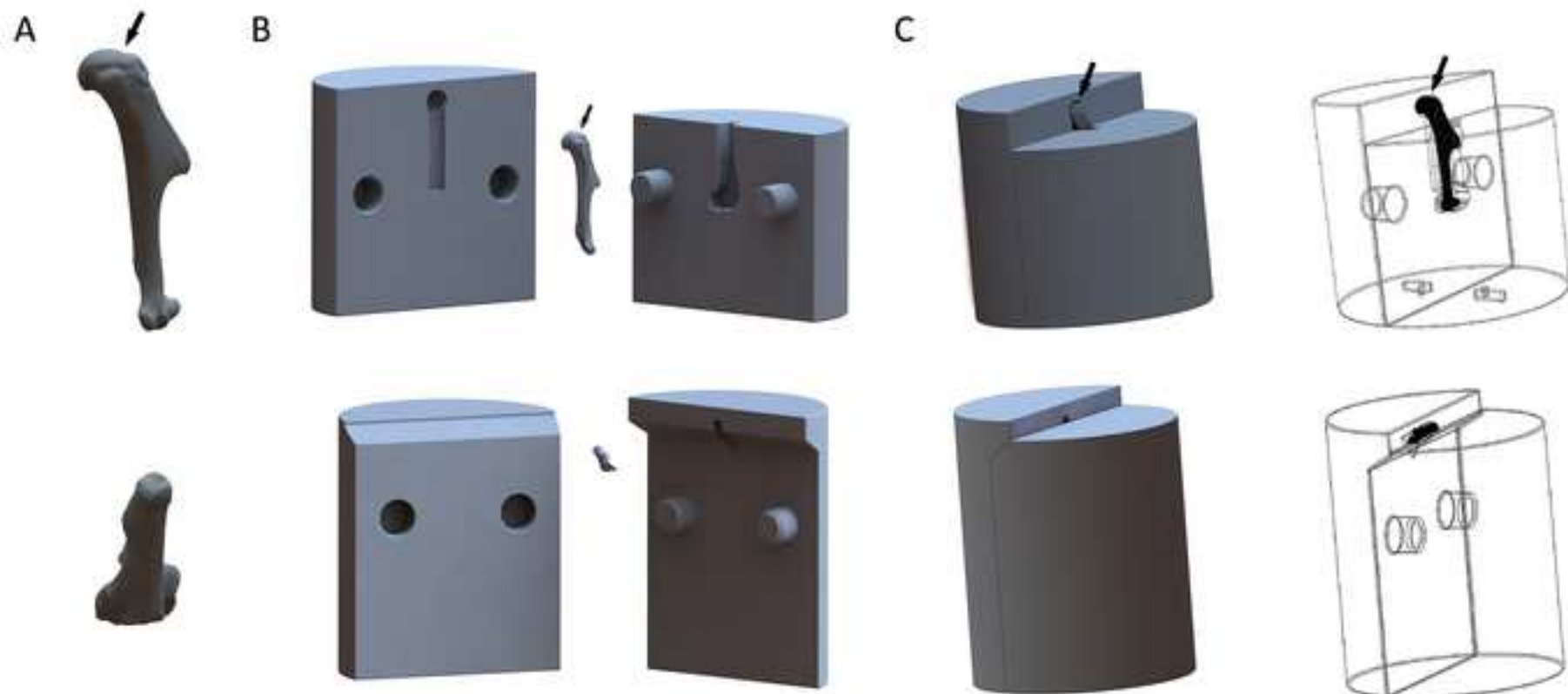
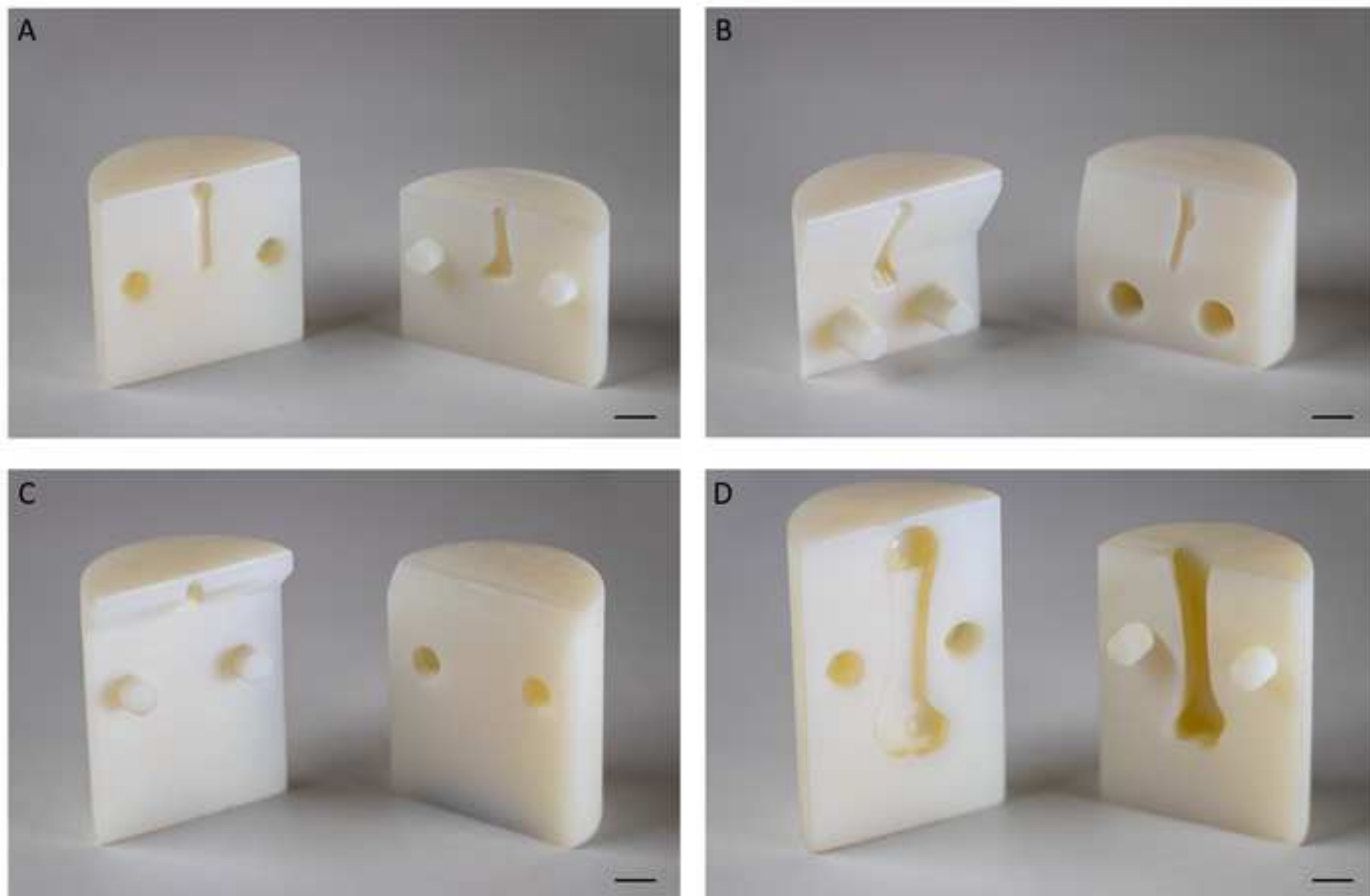
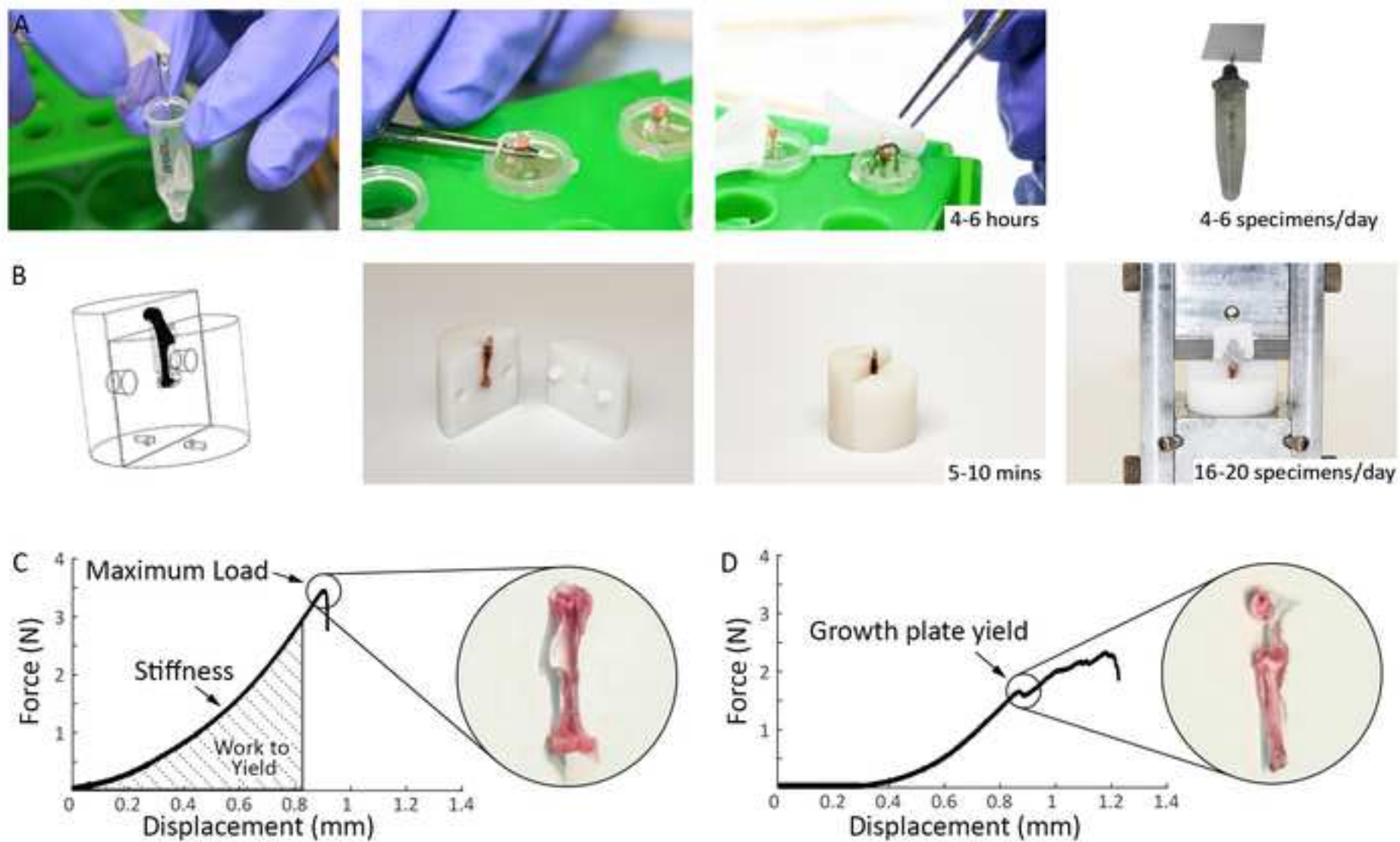


Figure 2

[Click here to access/download;Figure;Fig2.tif](#)





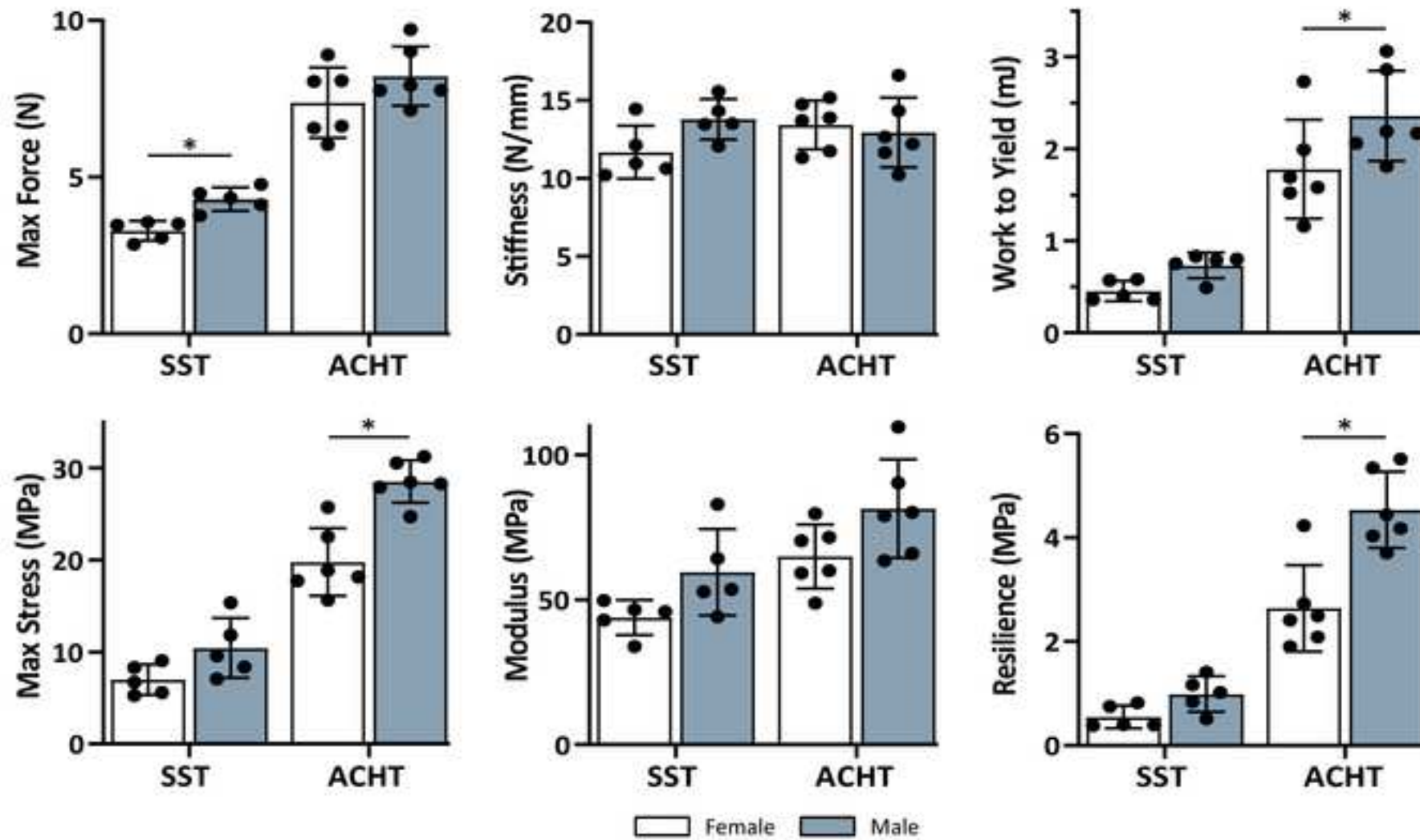
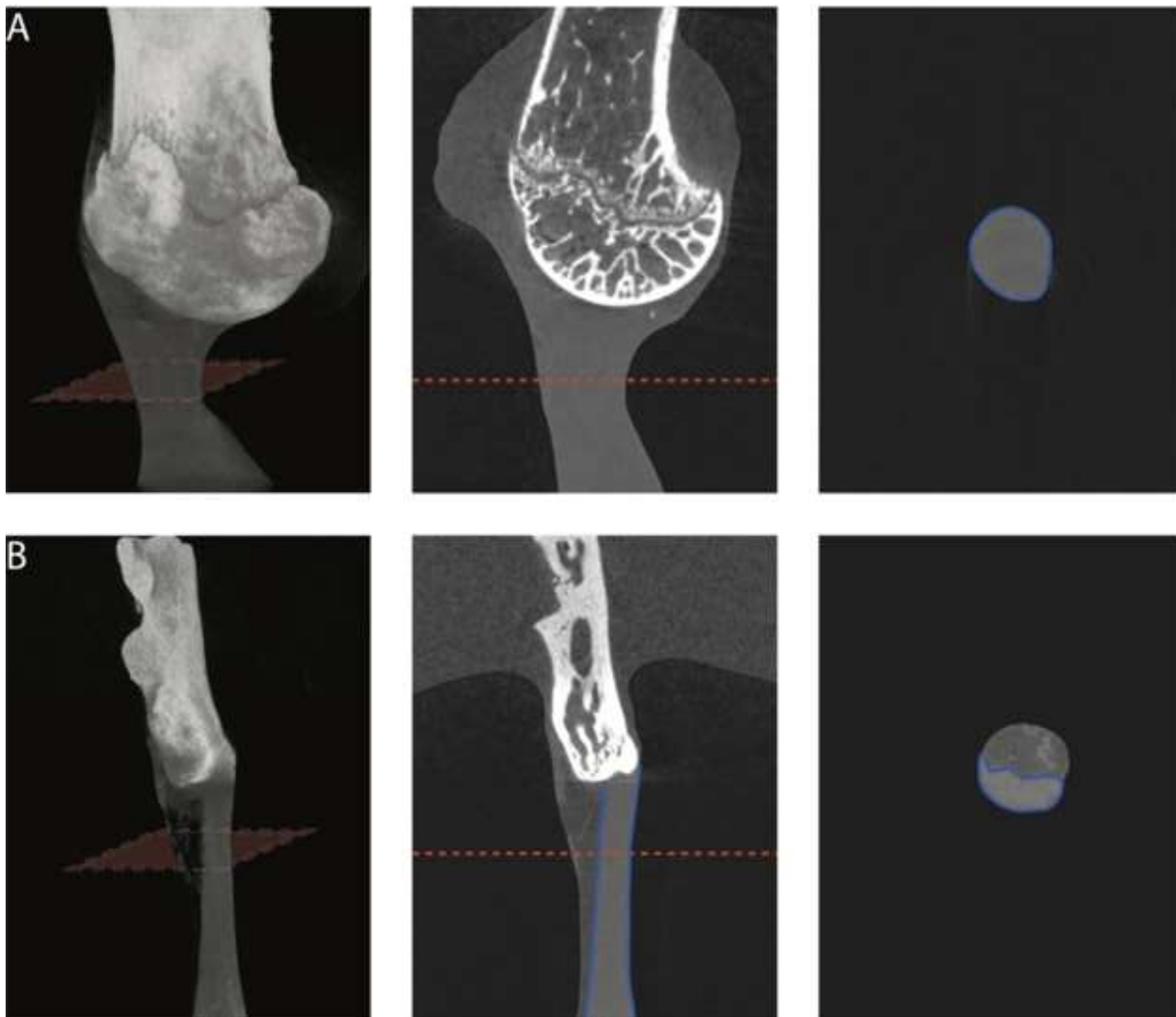


Figure 5



			Structura	
			Max Force (N)	
Author	N	Background	Mean \pm SD	COV(%)
Beason et al. <i>Journal of Shoulder and Elbow Surgery</i> (2013) ¹⁵	10	C57Bl/6	0.93 \pm 0.34	36.56
Bell et al. <i>Journal of Orthopaedic Research</i> (2014) ³¹	6	C57Bl/6	1.22 \pm 0.52	42.62
Cong et al. <i>Journal of Orthopaedic Research</i> (2018) ¹⁷	8	C57Bl/6	5.38 \pm 2.404 [#]	44.68
Connizzo et al. <i>Annals of Biomedical Engineering</i> (2014) ³²	10	NR (db/+)	NR	
Connizzo et al. <i>Journal of Biomedical Engineering</i> (2013) ¹⁴	NR	C57/BL6	NR	
Deymier et al. <i>Acta Biomaterialia</i> (2019) ²⁸	12	CD-1 IGS Mouse (WT)	5.0 \pm 0.7	14
Eekhoff et al. <i>Journal of Biomedical Engineering</i> (2017) ³³	13	Eln +/+	NR	
Killian et al. <i>FASEB Journal</i> (2016) ²⁹	8	C57BL/6	NR	
Schwartz et al. <i>Bone</i> (2014) ²⁵	20	CD-1 IGS Mouse (WT)	4.11 \pm 0.79*	19.22
Schwartz et al. <i>Development</i> (2015) ³⁰	12	(Rosa-DTA (DTA) x Gli1-CreERT2) ScxCre;Smofl/fl (WT)	4.16 \pm 0.29*	6.97
			Average COV	27.34
New Method	10	C57BL/6J	3.79 \pm 0.62	16.41

Mechanical Properties		Material Properties			
Stiffness (N/mm)		Max Stress (Mpa)		Modulus (MPa)	
Mean \pm SD	COV (%)	Mean \pm SD	COV (%)	Mean \pm SD	COV (%)
95.1 \pm 39.8 [†]	41.85	3.40 \pm 1.56	45.88	312.8 \pm 127.0	40.60
2.37 \pm 1.6	67.51	NR		NR	
4.25 \pm 1.67 [#]	39.29	NR		NR	
84.44 \pm 27.23 ^{*†}	32.25	NR		476 \pm 186.27 [*]	39.13
NR		NR		297 \pm 148.90 [*]	50.13
9.2 \pm 2.9	31.52	33 \pm 35	106.06	NR	
8.50 \pm 2.95	34.71	5.96 \pm 3.23	54.19	101.2 \pm 50.8	50.20
NR		7.79 \pm 2.61 [*]	33.50	58.32 \pm 31.73 [*]	54.41
8.58 \pm 3.78 [*]	44.06	12.29 \pm 5.95 [*]	48.41	133.80 \pm 59.41 [*]	44.40
11.04 \pm 1.98 [*]	17.93	26.24 \pm 5.81	22.14	121.89 \pm 44.18	36.25
Average COV	38.64	Average COV	51.70	Average COV	45.02
12.73 \pm 1.81	14.20	8.71 \pm 3.04	34.91	51.67 \pm 13.54	26.20

			Structural Properties		
			Max Force (N)		Stiffness (N)
Author	N	Background	Mean \pm SD	COV(%)	Mean \pm SD
Boivin et al. <i>Muscles, Ligaments and Tendons Journal</i> (2014) ¹⁹	6	Non-diabetic lean control mice	8.1 \pm 0.6	7.41	3.9 \pm 0.7
Connizzo et al. <i>Annals of Biomedical Engineering</i> (2014) ³²	10	db/+	NR		20.39 \pm 2.43*
Eekhoff et al. <i>Journal of Biomechanical Engineering</i> (2017) ³³	8	Eln +/+	NR		18.86 \pm 3.37
Mikic et al. <i>Journal of Orthopaedic Research</i> (2006) ³²	20	C57BL/6-J x 129SV/J	NR		NR
Probst et al. <i>Journal of Investigative Surgery</i> (2000) ²²	20	BALB/c	8.4 \pm 1.1	13.10	6.3 \pm 1.2
Shu et al. <i>Peer J</i> (2018) ²¹	9	C57BL/6	9.6 \pm 3.84	39.96	8.19 \pm 3.63
Sikes et al. <i>Journal of Orthopaedic Research</i> (2018) ³⁵	7	C57BL/6	NR		NR
Wang et al. <i>Journal of Orthopaedic Research</i> (2006) ³⁶	9	A/J	8.4 \pm 1.2	14.29	12.2 \pm 2.8
Wang et al. <i>Journal of Orthopaedic Research</i> (2006) ³⁶	8	C57BL/6J	10.2 \pm 1.4	13.73	13.1 \pm 2.5
Wang et al. <i>Journal of Orthopaedic Research</i> (2006) ³⁶	7	C3H/HeJ	12.5 \pm 1.7	13.60	14.1 \pm 3.2
Wang et al. <i>Journal of Orthopaedic Research</i> (2011) ³⁷	7	C57BL/6	6.6 \pm 1.7	25.76	8.2 \pm 1.4
Zhang et al. <i>Matrix Biology</i> (2016) ³⁸	NR	CD-1 and C57BL/6J	6.73 \pm 3.74*	55.57	12.03 \pm 3.34*
			Average COV	22.93	Average COV
New Method	12	C57BL/6J	7.8 \pm 1.08	13.91	13.19 \pm 1.86

	Material Properties			
/mm)	Max Stress (Mpa)		Young's modulus (MPa)	
COV (%)	Mean ± SD	COV (%)	Mean ± SD	COV (%)
17.95	NR		16 ± 3.7	23.13
11.92	NR		152.94 ± 44.12*	28.85
17.87	10.55 ± 2.97	28.15	443.8 ± 131.7	29.68
	18 ± 5	27.78	61 ± 20	32.79
19.05	NR		NR	
44.32	27.55 ± 10.54	38.26	NR	
	19.53 ± 7.03	0.36	62.82 ± 20.20	32.16
22.95	78.2 ± 8.6	11.00	713.9 ± 203.7	28.53
19.08	97.4 ± 11.4	11.70	765.1 ± 179.6	23.47
22.70	97.5 ± 10.9	11.18	708.6 ± 127.8	18.04
17.07	13.4 ± 3.7	27.61	86.8 ± 15.5	17.86
27.76	25.4 ± 15.14*	59.61	632.31 ± 113.79*	18.00
22.07	Average COV	23.96	Average COV	25.25
14.08	24.16 ± 5.42	22.45	73.17 ± 16.14	22.06

Name of Material/ Equipment

Agarose
Bruker microCT
ElectroForce
Ethanol 200 Proof
Fixture to attach grips
Kimwipes
MicroCT CT-Analyser (Ctan)
MilliQ water (Ultrapure water)
nTopology
Objet EDEN 260VS
Objet Studio
PBS - Phosphate-Buffered Saline
S&T Forceps
Scalpel Blade - #11
Scalpel Handle - #3
SkyScan 1272
Skyscan CT-Vox
SkyScan NRecon
SolidWorks CAD
SuperGlue
Testing bath
Thin film grips
VeroWhitePlus
WinTest

Company

Fisher Scientific
Bruker BioSpin Corp
TA Instruments
Fisher Scientific
Custom made
Kimberly-Clark
Bruker BioSpin Corp
Millipore Sigma
nTopology
Stratasys LTD
Stratasys LTD
ThermoFisher Scientific
Fine Science Tools
Fine Science Tools
Fine Science Tools
Bruker BioSpin Corp
Bruker BioSpin Corp
Bruker BioSpin Corp
Dassault Systèmes
Loctite
Custom made
Custom made
Stratasys LTD
WinTest Software

Catalog Number	Comments/Description
BP160-100	Dissove 1g in 100 ml ultrapure water to make 1% agarose
Skyscan 1272	Used by authors
3200	Testing platform
A4094	Dilute to 70% and use as suggested in protocol
	Used by authors
S-8115	As suggested in protocol
	Used by authors for visualizing and analyzing micro-CT scans
QGARD00R1 (or related purifier)	100 ml
Free 30 day trial	Engineering software for advanced manufacturing used by authors to refine mesh
	Precision Prototyping
	Used by authors with 3D printer
10010031	2.5 L of 10% PBS
00108-11	Used by authors
10011-00	Used by authors
10003-12	Used by authors
	Used by authors for visualizing and analyzing micro-CT scans
	Used by authors for visualizing and analyzing micro-CT scans
	Used by authors for visualizing and analyzing micro-CT scans
SolidWorks Research Subsription	Solid modeling computer-aided design used by authors
234790	As suggested in protocol
	Used by authors
	Used by authors
NA	3D printing material used by authors
	Used by authors to collect data

ARTICLE AND VIDEO LICENSE AGREEMENT

Title of Article:	Biomechanical testing of murine tendons
Author(s):	Iden Kurtaliaj, Mikhail Golman, Adam C. Abraham, Stavros Thomopoulos

Item 1: The Author elects to have the Materials be made available (as described at <http://www.jove.com/publish>) via:

☒ Standard Access ☐ Open Access

Item 2: Please select one of the following items:

- ☒ The Author is **NOT** a United States government employee.
- ☐ The Author is a United States government employee and the Materials were prepared in the course of his or her duties as a United States government employee.
- ☐ The Author is a United States government employee but the Materials were NOT prepared in the course of his or her duties as a United States government employee.

ARTICLE AND VIDEO LICENSE AGREEMENT

1. **Defined Terms.** As used in this Article and Video License Agreement, the following terms shall have the following meanings: **"Agreement"** means this Article and Video License Agreement; **"Article"** means the article specified on the last page of this Agreement, including any associated materials such as texts, figures, tables, artwork, abstracts, or summaries contained therein; **"Author"** means the author who is a signatory to this Agreement; **"Collective Work"** means a work, such as a periodical issue, anthology or encyclopedia, in which the Materials in their entirety in unmodified form, along with a number of other contributions, constituting separate and independent works in themselves, are assembled into a collective whole; **"CRC License"** means the Creative Commons Attribution-Non Commercial-No Derivs 3.0 Unported Agreement, the terms and conditions of which can be found at: <http://creativecommons.org/licenses/by-nc-nd/3.0/legalcode>; **"Derivative Work"** means a work based upon the Materials or upon the Materials and other pre-existing works, such as a translation, musical arrangement, dramatization, fictionalization, motion picture version, sound recording, art reproduction, abridgment, condensation, or any other form in which the Materials may be recast, transformed, or adapted; **"Institution"** means the institution, listed on the last page of this Agreement, by which the Author was employed at the time of the creation of the Materials; **"JoVE"** means MyJove Corporation, a Massachusetts corporation and the publisher of The Journal of Visualized Experiments; **"Materials"** means the Article and / or the Video; **"Parties"** means the Author and JoVE; **"Video"** means any video(s) made by the Author, alone or in conjunction with any other parties, or by JoVE or its affiliates or agents, individually or in collaboration with the Author or any other parties, incorporating all or any portion

of the Article, and in which the Author may or may not appear.

2. **Background.** The Author, who is the author of the Article, in order to ensure the dissemination and protection of the Article, desires to have the JoVE publish the Article and create and transmit videos based on the Article. In furtherance of such goals, the Parties desire to memorialize in this Agreement the respective rights of each Party in and to the Article and the Video.

3. **Grant of Rights in Article.** In consideration of JoVE agreeing to publish the Article, the Author hereby grants to JoVE, subject to **Sections 4** and **7** below, the exclusive, royalty-free, perpetual (for the full term of copyright in the Article, including any extensions thereto) license (a) to publish, reproduce, distribute, display and store the Article in all forms, formats and media whether now known or hereafter developed (including without limitation in print, digital and electronic form) throughout the world, (b) to translate the Article into other languages, create adaptations, summaries or extracts of the Article or other Derivative Works (including, without limitation, the Video) or Collective Works based on all or any portion of the Article and exercise all of the rights set forth in (a) above in such translations, adaptations, summaries, extracts, Derivative Works or Collective Works and (c) to license others to do any or all of the above. The foregoing rights may be exercised in all media and formats, whether now known or hereafter devised, and include the right to make such modifications as are technically necessary to exercise the rights in other media and formats. If the "Open Access" box has been checked in **Item 1** above, JoVE and the Author hereby grant to the public all such rights in the Article as provided in, but subject to all limitations and requirements set forth in, the CRC License.

ARTICLE AND VIDEO LICENSE AGREEMENT

4. **Retention of Rights in Article.** Notwithstanding the exclusive license granted to JoVE in **Section 3** above, the Author shall, with respect to the Article, retain the non-exclusive right to use all or part of the Article for the non-commercial purpose of giving lectures, presentations or teaching classes, and to post a copy of the Article on the Institution's website or the Author's personal website, in each case provided that a link to the Article on the JoVE website is provided and notice of JoVE's copyright in the Article is included. All non-copyright intellectual property rights in and to the Article, such as patent rights, shall remain with the Author.

5. **Grant of Rights in Video – Standard Access.** This **Section 5** applies if the "Standard Access" box has been checked in **Item 1** above or if no box has been checked in **Item 1** above. In consideration of JoVE agreeing to produce, display or otherwise assist with the Video, the Author hereby acknowledges and agrees that, Subject to **Section 7** below, JoVE is and shall be the sole and exclusive owner of all rights of any nature, including, without limitation, all copyrights, in and to the Video. To the extent that, by law, the Author is deemed, now or at any time in the future, to have any rights of any nature in or to the Video, the Author hereby disclaims all such rights and transfers all such rights to JoVE.

6. **Grant of Rights in Video – Open Access.** This **Section 6** applies only if the "Open Access" box has been checked in **Item 1** above. In consideration of JoVE agreeing to produce, display or otherwise assist with the Video, the Author hereby grants to JoVE, subject to **Section 7** below, the exclusive, royalty-free, perpetual (for the full term of copyright in the Article, including any extensions thereto) license (a) to publish, reproduce, distribute, display and store the Video in all forms, formats and media whether now known or hereafter developed (including without limitation in print, digital and electronic form) throughout the world, (b) to translate the Video into other languages, create adaptations, summaries or extracts of the Video or other Derivative Works or Collective Works based on all or any portion of the Video and exercise all of the rights set forth in (a) above in such translations, adaptations, summaries, extracts, Derivative Works or Collective Works and (c) to license others to do any or all of the above. The foregoing rights may be exercised in all media and formats, whether now known or hereafter devised, and include the right to make such modifications as are technically necessary to exercise the rights in other media and formats. For any Video to which this **Section 6** is applicable, JoVE and the Author hereby grant to the public all such rights in the Video as provided in, but subject to all limitations and requirements set forth in, the CRC License.

7. **Government Employees.** If the Author is a United States government employee and the Article was prepared in the course of his or her duties as a United States government employee, as indicated in **Item 2** above, and any of the licenses or grants granted by the Author hereunder exceed the scope of the 17 U.S.C. 403, then the rights granted hereunder shall be limited to the maximum

rights permitted under such statute. In such case, all provisions contained herein that are not in conflict with such statute shall remain in full force and effect, and all provisions contained herein that do so conflict shall be deemed to be amended so as to provide to JoVE the maximum rights permissible within such statute.

8. **Protection of the Work.** The Author(s) authorize JoVE to take steps in the Author(s) name and on their behalf if JoVE believes some third party could be infringing or might infringe the copyright of either the Author's Article and/or Video.

9. **Likeness, Privacy, Personality.** The Author hereby grants JoVE the right to use the Author's name, voice, likeness, picture, photograph, image, biography and performance in any way, commercial or otherwise, in connection with the Materials and the sale, promotion and distribution thereof. The Author hereby waives any and all rights he or she may have, relating to his or her appearance in the Video or otherwise relating to the Materials, under all applicable privacy, likeness, personality or similar laws.

10. **Author Warranties.** The Author represents and warrants that the Article is original, that it has not been published, that the copyright interest is owned by the Author (or, if more than one author is listed at the beginning of this Agreement, by such authors collectively) and has not been assigned, licensed, or otherwise transferred to any other party. The Author represents and warrants that the author(s) listed at the top of this Agreement are the only authors of the Materials. If more than one author is listed at the top of this Agreement and if any such author has not entered into a separate Article and Video License Agreement with JoVE relating to the Materials, the Author represents and warrants that the Author has been authorized by each of the other such authors to execute this Agreement on his or her behalf and to bind him or her with respect to the terms of this Agreement as if each of them had been a party hereto as an Author. The Author warrants that the use, reproduction, distribution, public or private performance or display, and/or modification of all or any portion of the Materials does not and will not violate, infringe and/or misappropriate the patent, trademark, intellectual property or other rights of any third party. The Author represents and warrants that it has and will continue to comply with all government, institutional and other regulations, including, without limitation all institutional, laboratory, hospital, ethical, human and animal treatment, privacy, and all other rules, regulations, laws, procedures or guidelines, applicable to the Materials, and that all research involving human and animal subjects has been approved by the Author's relevant institutional review board.

11. **JoVE Discretion.** If the Author requests the assistance of JoVE in producing the Video in the Author's facility, the Author shall ensure that the presence of JoVE employees, agents or independent contractors is in accordance with the relevant regulations of the Author's institution. If more than one author is listed at the beginning of this Agreement, JoVE may, in its sole

ARTICLE AND VIDEO LICENSE AGREEMENT

discretion, elect not take any action with respect to the Article until such time as it has received complete, executed Article and Video License Agreements from each such author. JoVE reserves the right, in its absolute and sole discretion and without giving any reason therefore, to accept or decline any work submitted to JoVE. JoVE and its employees, agents and independent contractors shall have full, unfettered access to the facilities of the Author or of the Author's institution as necessary to make the Video, whether actually published or not. JoVE has sole discretion as to the method of making and publishing the Materials, including, without limitation, to all decisions regarding editing, lighting, filming, timing of publication, if any, length, quality, content and the like.

12. **Indemnification.** The Author agrees to indemnify JoVE and/or its successors and assigns from and against any and all claims, costs, and expenses, including attorney's fees, arising out of any breach of any warranty or other representations contained herein. The Author further agrees to indemnify and hold harmless JoVE from and against any and all claims, costs, and expenses, including attorney's fees, resulting from the breach by the Author of any representation or warranty contained herein or from allegations or instances of violation of intellectual property rights, damage to the Author's or the Author's institution's facilities, fraud, libel, defamation, research, equipment, experiments, property damage, personal injury, violations of institutional, laboratory, hospital, ethical, human and animal treatment, privacy or other rules, regulations, laws, procedures or guidelines, liabilities and other losses or damages related in any way to the submission of work to JoVE, making of videos by JoVE, or publication in JoVE or elsewhere by JoVE. The Author shall be responsible for, and shall hold JoVE harmless from, damages caused by lack of sterilization, lack of cleanliness or by contamination due to

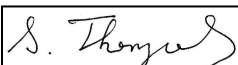
the making of a video by JoVE its employees, agents or independent contractors. All sterilization, cleanliness or decontamination procedures shall be solely the responsibility of the Author and shall be undertaken at the Author's expense. All indemnifications provided herein shall include JoVE's attorney's fees and costs related to said losses or damages. Such indemnification and holding harmless shall include such losses or damages incurred by, or in connection with, acts or omissions of JoVE, its employees, agents or independent contractors.

13. **Fees.** To cover the cost incurred for publication, JoVE must receive payment before production and publication of the Materials. Payment is due in 21 days of invoice. Should the Materials not be published due to an editorial or production decision, these funds will be returned to the Author. Withdrawal by the Author of any submitted Materials after final peer review approval will result in a US\$1,200 fee to cover pre-production expenses incurred by JoVE. If payment is not received by the completion of filming, production and publication of the Materials will be suspended until payment is received.

14. **Transfer, Governing Law.** This Agreement may be assigned by JoVE and shall inure to the benefits of any of JoVE's successors and assignees. This Agreement shall be governed and construed by the internal laws of the Commonwealth of Massachusetts without giving effect to any conflict of law provision thereunder. This Agreement may be executed in counterparts, each of which shall be deemed an original, but all of which together shall be deemed to be one and the same agreement. A signed copy of this Agreement delivered by facsimile, e-mail or other means of electronic transmission shall be deemed to have the same legal effect as delivery of an original signed copy of this Agreement.

A signed copy of this document must be sent with all new submissions. Only one Agreement is required per submission.

CORRESPONDING AUTHOR

Name:	Stavros Thomopoulos	
Department:	Orthopedic Surgery, Biomedical Engineering	
Institution:	Columbia University	
Title:	Professor	
Signature:		Date: 5/16/19

Please submit a **signed** and **dated** copy of this license by one of the following three methods:

1. Upload an electronic version on the JoVE submission site
2. Fax the document to +1.866.381.2236
3. Mail the document to JoVE / Attn: JoVE Editorial / 1 Alewife Center #200 / Cambridge, MA 02140

BIOMECHANICAL TESTING OF MURINE TENDONS

Iden Kurtaliaj, Mikhail Golman, Adam C. Abraham, Stavros Thomopoulos

Response to reviewers

We would like to thank the reviewers and editor for their critical review of our manuscript. Our responses to their specific comments are provided below.

Editorial comments:

General:

1. Please take this opportunity to thoroughly proofread the manuscript to ensure that there are no spelling or grammar issues.

Response: *We have thoroughly proofread the manuscript to correct any spelling or grammar issues.*

2. Please ensure that the manuscript is formatted according to JoVE guidelines—letter (8.5" x 11") page size, 1-inch margins, 12 pt Calibri font throughout, all text aligned to the left margin, single spacing within paragraphs, and spaces between all paragraphs and protocol steps/substeps.

Response: *We have carefully edited and formatted the manuscript according to JoVE guidelines.*

3. JoVE cannot publish manuscripts containing commercial language. This includes trademark symbols (™), registered symbols (®), and company names before an instrument or reagent. Please limit the use of commercial language from your manuscript and use generic terms instead. All commercial products should be sufficiently referenced in the Table of Materials and Reagents. For example: SkyScan, CTAn, SolidWorks, VeroWhitePlus, Kimwipe, ElectroForce, Eppendorf.

Response: *We apologize for the use of commercial language in the manuscript. We have edited the text to read:*

*"1.1.2 Perform a microcomputed tomography scan of the entire bone, e.g., scan the humerus and calcaneus samples. NOTE: Depending on the scanner used, the settings will be different. For the scanner used in the current study (see **Table of Materials**), the recommended settings are: scan at an energy of 55 kVP, Al 0.25 filter, at a resolution of 6 μm ."*

"1.1.3 Reconstruct microcomputed tomography scan projection images into cross-section images. Use recommended parameters for the experimenter's scanner/software

combination. NOTE: For the program used in the current study (see **Table of Materials**) it is recommended to use the following reconstruction parameters: Smoothing: 0-2, Beam Hardening Correction: 45, Ring Artefact Reduction: 4-9 and to reconstruct slices in 16-bit TIFF format.”

“1.1.4 Create a 3D surface model and save into a standard STL format compatible with most 3D printers and rapid prototyping. NOTE: For the program used in the current study (see **Table of Materials**) it is recommended to:”

“1.1.6.1 Manipulate the mesh to reduce the size of the STL file and make it compatible with any solid modeling computer-aided design program. NOTE: For the program used in the current study (see **Table of Materials**), it is recommended to follow the steps below:

1.1.6.1.1 Choose “Refine Mesh”, from the toolset Utilities.

1.1.6.1.2 Select the mesh object to edit.

1.1.6.1.3 Reduce mesh by a factor of 0.95 to lower the end size of the mesh object. NOTE: the “Remesh” tool could also be used to reduce the size of the mesh.

1.1.6.1.4 Resave the newly reduced file in STL format by choosing “Export as...”.

“1.2.1.1 Use a solid modeling computer-aided design program to create a custom-fit model of humerus gripping fixture (Fig. 1). NOTE: The program used in the current study is listed in the **Table of Materials**.”

“NOTE: The printer used in the current study uses PolyJet technology (see **Table of Materials**). It prints a 16 μ m layer of liquid ultraviolet curable photopolymer and then cures it by ultraviolet laser to solidify the pattern. The material used in the current study has a modulus of 2.5 GPa.”

“2.1.2 Determine the cross-sectional area of the tendon using microcomputed tomography. NOTE: For the scanner used in the current study (see **Table of Materials**), the recommended settings are: scan at an energy of 55 kVP, Al 0.25 filter, at a resolution of 5 μ m.”

“2.1.5 Insert and glue tendon between a folded thin tissue paper (2 x 1 cm) and clamp the construct using thin film grips.”

“2.2.1 Perform tensile mechanical test on a materials testing frame. NOTE: For the testing frame used in the current study (see **Table of Materials**), the recommended protocol is:”

“2.2.9 After completion of tensile testing, perform a microcomputed tomography scan. NOTE: For the scanner used in the current study (see **Table of Materials**), the recommended settings are: scan at an energy of 55 kVP, Al 0.25 filter, at a resolution of 12.3 μ m.”

“2.2.10 Repeat step 1.1.3.

*2.2.10 Use a 3D visualization program compatible with your scanner to create a volume rendered 3D model of the scanned object. NOTE: The program used in the current study is listed in the **Table of Materials**.*

2.2.11 Determine failure mode and failure site area by inspecting the 3D object.”

“First, step 1.1.2 is necessary to create a 3D model of the desired bone; however, due to the typically high resolution used for this scan, the file size may be too large to use with solid modeling programs. The software used in this protocol successfully reduced the size of the file (step 1.1.8.2) and preserved object geometry, although other softwares may also be effective to achieve this.”

“To measure the cross-sectional area of the supraspinatus tendon, we recommend microcomputed tomography scans of the bone-tendon-muscle specimen suspended in a cryotube with a flat bottom, where the bone is held upside down in the tube with agarose.”

“For the Achilles tendon, high resolution microcomputed tomography scans reveal two distinct tissues when examined: the tendon proper and the surrounding sheath, which appears as a lighter shade.”

Protocol:

1. There is a 10 page limit for the Protocol, but there is a 2.75 page limit for filmable content. If revisions cause the highlighted portion to be more than 2.75 pages, please highlight 2.75 pages or less of the Protocol (including headers and spacing) that identifies the essential steps of the protocol for the video, i.e., the steps that should be visualized to tell the most cohesive story of the Protocol.

Response: *We have highlighted 2.75 pages of our protocol for filmable content, identifying the essential steps.*

2. Please add more details to your protocol steps. Please ensure you answer the “how” question, i.e., how is the step performed? Alternatively, add references to published material specifying how to perform the protocol action. If revisions cause a step to have more than 2-3 actions and 4 sentences per step, please split into separate steps or substeps.

Response: *We edited protocol steps 1.1.1, 2.1.1, 1.1.2-1.1.6, 1.2.1, and 2.2.2-2.2.13, and added references to steps 2.2.6-2.2.7, 2.2.13.*

Specific Protocol steps:

1. 1.1.1, 2.1.1: Please provide details for how these bones (and tendons) are obtained and dissected.

Response: We thank the editors for the suggestion. We now provide a more detailed description of how to isolate muscle - tendon - bone specimens for testing (specifically, supraspinatus muscle - tendon - humerus bone and gastrocnemius muscle - Achilles tendon - calcaneus bone). The protocol was edited to read as follows:

“1.1.1 Dissect the bone of interest in preparation for 3D model creation and 3D bone grip printing; the humerus and the calcaneus are used as examples in the current protocol. NOTE: Detailed instructions to dissect bone-tendon-muscle specimens for mechanical testing are provided in step 2.1.1. The following steps should be followed to isolate bones for the purpose of creating 3D-printed bone grips.

1.1.1.1 Dissection of the humerus: after sacrifice, remove upper extremity skin, remove all muscles over the humerus, disarticulate the elbow and glenohumeral joints, and carefully remove all connective tissues attached to the humerus.

1.1.1.2 Dissection of the calcaneus: after sacrifice, remove lower extremity skin, disarticulate the Achilles tendon-calcaneus joint and joints between calcaneus and other foot bones, and carefully remove all connective tissues attached to the calcaneus.”

2.1.1 Dissect the muscle-tendon-bone of interest in preparation for tensile mechanical testing. In the current study, supraspinatus muscle - tendon - humerus bone specimens (N=10, 5 male, 5 female) and gastrocnemius muscle - Achilles tendon-calcaneus bone specimens (N=12, 6 male, 6 female) were isolated from 8 week old C57BL/6J mice.

2.1.1.1 Dissection of the supraspinatus muscle - tendon - humerus bone specimen

2.1.1.1.1 After sacrifice, position the mouse in a prone position.

2.1.1.1.2 Make an incision in the skin from above the elbow of the forepaw towards the shoulder.

2.1.1.1.3 Carefully remove the skin with blunt dissection so that the musculature of the shoulder is visible.

2.1.1.1.4 Remove the tissue surrounding the humerus until the bone is exposed and can be held securely with forceps.

2.1.1.1.5 Hold the humerus with forceps and carefully remove the deltoid and trapezius muscles to expose the coracoacromial arch.

2.1.1.1.6 Identify the acromioclavicular joint and carefully separate the clavicle from the acromion with a scalpel blade.

2.1.1.1.7 Taking care not to damage the supraspinatus tendon and its bony attachment, remove the muscle from its scapular attachment using a scalpel blade.

2.1.1.1.8 Taking care not to damage the supraspinatus tendon and its bony attachment, detach the humeral head from the glenoid; using a scalpel blade, lacerate the joint capsule and the infraspinatus, subscapularis, and teres minor tendons.

2.1.1.1.9 Disarticulate the elbow joint to separate the humerus from the ulna and radius.

2.1.1.1.10 Isolate the humerus - supraspinatus tendon - muscle specimen and clean off excess soft tissues on the humerus and humeral head.

2.1.1.2 Dissection of the Achilles tendon - calcaneus bone sample

2.1.1.2.1 After sacrifice, position the mouse in a supine position.

2.1.1.2.2 Taking care not to damage the Achilles tendon and its bony attachment, remove the skin with blunt dissection so that the musculature around the ankle and knee joints is exposed.

2.1.1.2.3 Using a scalpel blade, starting at the Achilles tendon - calcaneus attachment, carefully detach the gastrocnemius muscle from its proximal attachments.

2.1.1.2.4 Carefully disarticulate the calcaneus from the various adjacent bones.

2.1.1.2.5 Isolate the Achilles tendon - calcaneus specimen and clean off excess soft tissues.

2. 1.1.2-1.1.17, 1.2.1, 2.2.2-2.2.9: Please provide more detailed instructions for how to carry out these software steps, in particular for any step you intend to have filmed.

Response: We agree that more detailed instructions are needed. For each of the steps mentioned, we have edited the text to read as follows:

1.1.2-1.1.7

Response:

"1.1.2 Perform a microcomputed tomography scan of the entire bone, e.g., scan the humerus and calcaneus samples. NOTE: Depending on the scanner used, the settings will be different. For the scanner used in the current study (see **Table of Materials**), the recommended settings are: scan at an energy of 55 kVP, Al 0.25 filter, at a resolution of 6 μm .

1.1.2.1 Mix agarose powder in ultrapure water and microwave for 1-3 min until the agarose is completely dissolved. NOTE: It is helpful to microwave for 30-45 sec, stop and swirl, and then continue towards a boil.

1.1.2.2 Fill cryotubes up to $\frac{3}{4}$ with agarose.

1.1.2.3 Let the agarose cool for about 5-10 minutes.

1.1.2.4 Insert bone into the agarose gel (this will prevent movement artifacts during scanning).

1.1.2.5 Insert cryotube with bone into the scanner. NOTE: For the scanner used in the current study, a 16-position automatic sample changer was used for all scans. This scanner can automatically select magnification according to a sample's size and shape.

1.1.3 Reconstruct microcomputed tomography scan projection images into cross-section images. Use the recommended parameters for the particular scanner/software

combination. NOTE: For the program used in the current study (see **Table of Materials**) it is recommended to use the following reconstruction parameters: Smoothing: 0-2, Beam Hardening Correction: 45, Ring Artefact Reduction: 4-9 and to reconstruct slices in 16-bit TIFF format.

1.1.4 Create a 3D surface model and save into a standard STL format compatible with most 3D printers and rapid prototyping. NOTE: For the program used in the current study (see **Table of Materials**) it is recommended to:

1.1.4.1 Open file dataset. From the menu select the command File / Open.

1.1.4.2 Open the dialog File / Preferences and select the tab "Advanced".

1.1.4.1 Use the double-time cubes algorithm to construct the 3D models. This algorithm minimizes the number of facet triangles and provides smoother surface detail.

1.1.4.2 Use 10 as the locality parameter; this parameter defines the distance in pixels to the neighboring point used for finding the object border.

1.1.4.3 Minimize tolerance to 0.1 to decrease file size.

1.1.4.3 NOTE: After opening the dataset, the images are shown in the "Raw Images" page.

1.1.4.4 To specify the volume of interest (VOI), manually select two images to set as the top and bottom of the selected VOI range.

1.1.4.5 Move to the second page "Region of Interest". Manually select the region of interest on a single cross section image. NOTE: The selected region will be highlighted in red (i.e. the humerus cross-sectional area).

1.1.4.6 Repeat previous step every 10-15 cross-section images.

1.1.4.7 Move to the third page "Binary Selection".

1.1.4.8 On the histogram menu click "From dataset". The histogram distribution of brightness from all images of the dataset will be shown.

1.1.4.9 Also on the histogram menu, click the "Create a 3D Model" file menu.

1.1.4.10 Save 3D model of bone in STL file format."

1.2.1

Response:

"1.2.1 Supraspinatus tendon-humeral bone

1.2.1.1 Use a solid modeling computer-aided design program to create a custom-fit model of humerus gripping fixture (Fig. 1). NOTE: The program used in the current study is listed in the **Table of Materials**."

1.2.1.2 Open the STL format file of the humerus bone in a solid modeling program and save as a part file. NOTE: For the software used in the current study (see **Table of Materials**) the 3D bone object was saved in SLDPRT format.

1.2.1.3 Open the part file and manually create three anatomically relevant planes (i.e sagittal, coronal, transverse)

1.2.1.3.1 Manually define the sagittal plane to cut through the supraspinatus tendon attachment at the greater tuberosity.

1.2.1.3.2 Ensure that the 3D block contains the sagittal plane as a plane of symmetry. To achieve this add or cut material from the block if needed. NOTE: This plane of symmetry ensures that when the specimen is inserted into the fixtures the tendon and tendon attachment are located in the central axis of the fixture.

1.2.1.4 Measure dimensions of the bone along each of the three planes (i.e., height, width, length).

1.2.1.5 Measure the dimensions of the mechanical testing grips where the 3D printed fixture will be attached.

1.2.1.6 Begin with designing a solid block part (e.g., a solid cylinder).

1.2.1.6.1 Ensure that each dimension of the block is at least 5 mm greater than the dimensions of the humerus.

1.2.1.6.1 Account for design constraints from mechanical testing grips (i.e., ensure that the 3D printed fixture can be assembled and disassembled freely in the mechanical testing grips).

1.2.1.7 Create an assembly model with two components: the solid block and either the right or left humerus bone.

1.2.1.8 Define the orientation of the bone within the block (i.e., the angle between the tendon and bone).

1.2.1.9 Ensure that the entire bone volume fits inside the block.

1.2.1.10 Create a cavity in the block using the humerus bone as the mold. NOTE: In the current study, using the software specified in the **Table of Materials**, it is recommended to follow the steps below:

1.2.1.10.1 Insert the design part (humerus) and the mold base (cylinder block) into an interim assembly.

1.2.1.10.2 In the assembly window, select the block, and click Edit Component on the Assembly toolbar.

1.2.1.10.3 Click Insert → Mold → Cavity.

1.2.1.10.4 Select Uniform scaling and enter 0% as the value to scale in all directions.

1.2.1.11 Cut the assembly along the sagittal plane to create two symmetrical components that fit the bone anteriorly and posteriorly (e.g., two half cylinders, as seen in Figure. 1). NOTE: Two components are designed that fit the bone anteriorly and posteriorly. The anterior component includes a half spherical-shaped cavity extended from the anterior side of the humeral head up to the supraspinatus tendon attachment. The posterior component cavity is shaped like the posterior part of the humerus (i.e., posterior side of the humeral head, deltoid tuberosity, and medial and lateral epicondyle)

1.2.1.12 Save each component as a separate file part.

1.2.1.13 For the anterior component, ensure that the humeral head is embedded in the cavity of the part by defining appropriate tolerances. NOTE: In the current study, using the software specified in the **Table of Materials**, it is suggested to follow the steps below:

1.2.1.13.1 Create a revolved cut to smooth the mesh geometry of the cavity.

1.2.1.13.2 Create a sketch for the cut by emulating the cavity geometry and adding a locational clearance. NOTE: The clearance allows for free assembly and disassembly between the bone and the anterior component.

1.2.1.14 Modify the posterior component to imitate the cavity geometry to create a cut that adds clearance, as described above for the anterior component.

1.2.1.15 Make a cut in the transverse plane starting from the top of the posterior component up to the crest of the greater/lesser tubercle. NOTE: As seen in Figures 1 and 2, the posterior component includes a cut that creates an opening at the tendon attachment.

1.2.1.16 Create a snug fit between the two components to allow for free assembly and disassembly. NOTE: A hole-shaft fit with a loose running clearance was created for the fixtures in the current study.

1.2.1.17 Create 3D mirror models for each component of the fixture for the opposite limb (i.e., left or right).

1.2.1.18 Add an etch on the bottom of the fixtures to distinguish between the left and right sides.

1.2.1.19 Save all fixture parts in STL standard file format in preparation for 3D printing."

2.2.2-2.2.9

Response:

"2.2.2. Collect load-deformation data.

2.2.3. Calculate strain as displacement relative to the initial gauge length of the tendon.

2.2.3.1 Use calipers to measure gauge length from attachment site to tendon grips.

2.2.4. Calculate stress as force divided by initial tendon cross-sectional area (as measured from microCT).

2.2.5. If interested in viscoelastic behavior, a stress relaxation can be performed prior to the tension test to failure and the data can be used to calculate parameters such as A, B, C, tau1, and tau2 from the quasilinear viscoelastic model²⁴.

2.2.6. From the load deformation curve, calculate stiffness (i.e., the slope of the linear portion of curve), maximum force, and work to yield (i.e., the area under the curve up to yield force).

2.2.6.3 Identify the linear portion by choosing a window of points in the load-deformation curve that maximizes the R^2 value for a linear least squares regression²⁵.

2.2.6.1 Determine the stiffness as the slope of the linear portion of the load-displacement curve^{25,26}.

2.2.7. From the stress strain curve, calculate modulus (i.e., the slope of the linear portion of curve), strength (i.e., maximum stress), and resilience (i.e., the area under the curve up to yield stress).

2.2.8 NOTE: Using the RANSAC algorithm in Matlab (The Mathworks, Natick, MA), the yield strain (x-value) is defined as the first point when the y-fit has deviated more than 0.5% of the expected stress value (y-value). Yield stress is the corresponding y-value of yield strain.

2.2.9 NOTE: In addition to the monotonic tensile loading to failure described in the current study, cyclic loading can provide important information about tendon fatigue and/or viscoelastic properties. For example, Freedman et al reported fatigue properties of murine Achilles tendons.²⁷

2.2.10 After completion of tensile testing, perform a microcomputed tomography scan of the entire bone, e.g., scan the humerus and calcaneus samples. NOTE: For the scanner used in the current study (see **Table of Materials**), the recommended settings are: scan at an energy of 55 kVP, Al 0.25 filter, at a resolution of 6 μm .

2.2.10.1 Repeat steps 1.1.2.1 - 1.1.2.5

2.2.11 Repeat step 1.1.3

2.2.12 Use a 3D visualization program compatible with the scanner to create a volume-rendered 3D model of the scanned object. NOTE: The program used in the current study is listed in the **Table of Materials**."

2.2.13 Determine the failure mode and failure site area by inspecting the 3D object."

Figures:

1. Please cite Figure 4 outside of the Figure Legends section.

Response: We thank the editors for pointing out that Figure 4 was not cited outside of the Figure Legends section. We have corrected the text to read:

"Animal sex had a significant effect on the mechanical properties of the supraspinatus and Achilles tendons (Figure. 4)."

2. Figure 3A, B: Please include more information about what is shown here in the legend.

Response: We have corrected the text to read:

"Figure 3: Comparison of previous and current methods for mechanical testing of murine supraspinatus tendons. (A) Previous specimen preparation methods used in our laboratory prior to mechanical testing: the humerus was potted in epoxy up to the humeral head to stabilize the bone, a paper clip was placed over the humeral head to prevent growth plate fracture, and, for the epoxy to cure, the specimens were left in room temperature for 4-6 hours prior to mechanical testing. (B) Specimen preparation methods used in the current study (Steps 1.2-1.3 and 2.1.4-2.1.6): Top left shows a 3D representation of the fixtures as produced by a solid modeling program. The 3D printed fixtures are reusable and easily assembled and disassembled. The bone end of the specimen is inserted into the fixtures, securing the growth plate and exposing the tendon for gripping and testing. The tendon end is glued between a folded thin tissue paper and inserted into the grips. Preparation time for each specimen is 10-15 minutes. (C) Representative load-deformation curves for tensile testing of a supraspinatus tendon

using methods described in the current study. (D) Representative load-deformation curve for tensile testing of supraspinatus tendon using prior methods, showing a growth plate failure."

References:

1. Please do not abbreviate journal titles.

Response: *We have corrected the references according to JoVE formatting requirements.*

Table of Materials:

1. Please ensure the Table of Materials has information on all materials and equipment used, especially those mentioned in the Protocol.

Response: *We have corrected the Table of Materials to include all materials.*

Reviewers' comments:

Reviewer #1:

Manuscript Summary:

A new system is developed for murine tendon mechanical testing.

Major Concerns:

None.

Response: *We thank the reviewer for the careful review of our manuscript.*

Minor Concerns:

It is stated (lines 54-55) that "few studies have tested the biomechanical properties of murine tendons" and that (line 280) "mechanical properties is... rarely reported". Then the authors (line 325) state they reviewed 20 studies which did so which is a reasonable body of literature (not few or rare) for something only done relatively recently.

Response: *We thank the reviewer for noting this ambiguity and agree the testing of murine tendons is becoming more common. We have replaced "rarely reported" with "uncommon". Notably, in the last 20-30 years, major advancements in tendon research have rapidly increased this body of literature. In the last decade alone, according to PubMed, there were 1595 published peer-reviewed journal articles on tendon. 823 of these studies used murine models (~52%). However, only 6% of these murine papers reported tendon mechanical properties. As discussed in the manuscript, we believe that this small percentage is due to the difficulty in gripping these small tissues, tedious and time-consuming specimen preparation methods, and artifactual growth plate fractures.*

The mechanical properties described (lines ~185-191) are just the simplest. For completeness and guidance to the reader, it should be noted that fatigue testing and/or frequency sweeps can often be beneficial.

Response: *This is an excellent point. We agree that cyclic loading of tendon can provide important information about tendon fatigue and/or viscoelastic properties. We have added step 2.2.9 to read:*

“NOTE: In addition to the monotonic tensile loading to failure described in the current study, cyclic loading can provide important information about tendon fatigue and/or viscoelastic properties. For example, Freedman et al reported fatigue properties of murine Achilles tendons.²⁷”

The potential upscale to larger animal models (345) should acknowledge the potential of compliance of the 3D printed fixture material (depending on material) which is likely not an issue with the low loads of murine tendons).

Response: *We agree that the modulus of the 3D printed fixture material must be high enough that it is not compliant relative to the strength of the tendon being tested. Using standard plastic materials to 3D print these fixtures is cost effective and appropriate for testing both murine and rat tendons. We have not validated the fixtures for larger animals, and agree that compliance could become an issue. Testing of tendons from larger animals may require metal 3D printing, which is considerably more expensive. The edited text now reads (line 516):*

“Furthermore, these methods are not limited to the supraspinatus and Achilles tendons, as they are easily adapted to testing other murine tendons and tendons from larger animal models. To test tendons from larger animals, however, the modulus of the 3D printed fixture material must be high enough that it is not compliant relative to the strength of the tendon being tested.”

Reviewer #2:

Manuscript Summary:

The manuscript describes a new way to test ligaments and tendons of murine models. The group 3D prints a sample grip using micro CT scans of the bone that the tissue is attached to. This creates more uniform gripping at the base of the sample. This mounting procedure reduces preparation time, limit sample slippage, prevent tearing at the grips, and reduce variations between samples.

Response: *We thank the reviewer for the careful review of our manuscript.*

Major Concerns:

Does a new grip need to be made for every sample. If you want the best possible grip it is assumed that every sample would have its own custom grip. Printing them may not be expensive, but scanning the samples for the printing requirements could get expensive.

Response: We thank the reviewer for raising these important points. Our point by point responses to the reviewer are as follows:

Does a new grip need to be made for every sample.

Response: It is not necessary to make a new grip for every sample. The grips are reusable (there is no glue or epoxy in the fixture; the bone is held in a press fit). Furthermore, small variations from sample to sample do not affect the effectiveness of the fixtures. For the design of the fixtures in the current study, we scanned each bone once (i.e., left humerus, right humerus, and calcaneus) and created one 3D model for each bone. We then used the three fixtures to conduct all mechanical testing for this manuscript.

If you want the best possible grip it is assumed that every sample would have its own custom grip.

Response: For animals of the same age, the bone geometry is nearly identical, thus the same fixture can be used for testing of all specimens. In this manuscript, we used 8-week old mice (skeletally mature adult mice) and 3D printed fixtures specific to this age group to test tendons. It was not necessary to create separate male and female fixtures. For other age groups (e.g., 4-week mice) or mice with unique bone phenotypes it is recommended that fixtures that fit the particular geometries of the bones are manufactured.

Printing them may not be expensive, but scanning the samples for the printing requirements could get expensive.

Response: As the fixtures are reusable, only one scan is needed for any particular group. Additional fixtures can be printed based on the scan, as needed.

We have clarified the above points in the revised paper (steps: 2.1.4, 475-483).

Minor Concerns:

Perhaps the protocol would be better suited for a chart?

Response: Figure 3 summarizes the protocol for specimen preparation prior to mechanical testing, comparing previous methods to the new method. Although this is not a chart, we now provide more detail in the figure's legend. For the detailed protocol, we followed the required format of JoVE, and note that the final publication will also include the key parts of the protocol in an instructional video.

How were the COV and average calculated?

Response: We summarized mean \pm standard deviation for each of the mechanical properties (i.e., maximum force, stiffness, maximum stress, and modulus), as reported from all cited studies (Tables 1 and 2). COV was calculated by dividing the standard deviation by the mean. The mean of the COVs was then determined to provide a measure of typical variation in published methods.

It could be said that the first 3 studies are driving up the average COV for the other studies.

Response: Thank you for identifying this. We conducted a literature research and included all studies that determined the mechanical properties of the murine supraspinatus tendon. Although the first three studies have higher COVs than some of the other reports, we note that they were conducted by three different laboratories. Furthermore, all COVs are included in the table, so the reader can compare the current results to individual prior studies as well as to the mean COV from prior studies.

Would it further improve the outcome if the bone was epoxied into the printed part or if it was roughened on the inside?

Response: We thank the reviewer for the suggestion. Because the fixtures are printed at a relatively high resolution accurately reflecting the bone geometry, epoxy is not necessary. Use of epoxy may indeed marginally improve fixation, but this would be at the cost of substantial additional preparation time and the inability to reuse the fixture. Roughening the inner surface of the fixture may also improve fixation, but would be difficult to implement and the expected benefit would be marginal.

This work seems like a methods paper.

Response: Although we present data on the effect of sex on murine tendon mechanical properties, the paper is indeed primarily a methods paper. This is consistent with the goals of JoVE: "JoVE publishes the leading peer-reviewed, PubMed-indexed video methods journal. Articles consist of high-quality video demonstrations and detailed text protocols which facilitate scientific reproducibility and productivity. The scope of the journal includes novel techniques, innovative applications of existing techniques, and gold standard protocols in the physical and life sciences."

It would be more convincing if the group tested samples using the epoxy method as well as the custom grip method that they designed.

Response: We thank the reviewer for bringing up this valuable point. The last three studies from our laboratory (Table 1) used the epoxy method to determine the mechanical properties of murine supraspinatus tendons. Other groups use similar approaches and none of them use 3D printed fixtures. Therefore, a direct comparison can be made with the results using the current methods and the prior methods from our

group and others, as presented in Table 1.

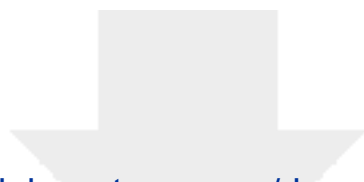


[Click here to access/download](#)

Supplemental Coding Files

Part1_60degreeswithcavity_0.8mmtallwall.STL

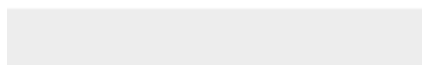
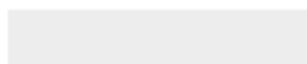


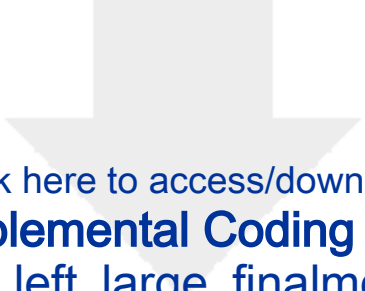


[Click here to access/download](#)

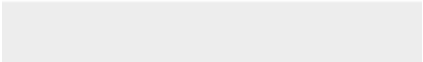
Supplemental Coding Files

Part2_60degreeswithcavity_addedtaper and etch.STL





Click here to access/download
Supplemental Coding Files
Part_2_left_large_finalmod.STL





[Click here to access/download](#)

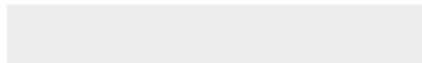
Supplemental Coding Files

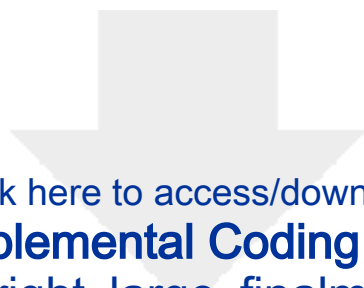
Part_2_right_bone_mod_inchod.STL



[Click here to access/download](#)

Supplemental Coding Files
Part1_left_large_finalmod.STL





[Click here to access/download](#)

Supplemental Coding Files

Part1_right_large_finalmod.STL

